UNIVERSIDAD TECNICA FEDERICO SANTA MARIA

Repositorio Digital USM **https://repositorio.usm.cl**

Departamento de Arquitectura Arq_paso

2021-11-23

MODELING AND CONTROL OF PIEZOELECTRIC ACTUATORS: AN IRREVERSIBLE PORT-HAMILTONIAN APPROAC

CABALLERÍA MAGNA, JAVIER ALEJANDRO

https://hdl.handle.net/11673/52770

Repositorio Digital USM, UNIVERSIDAD TECNICA FEDERICO SANTA MARIA

Universidad Técnica Federico Santa María
Departamento de Electrónica
Valparaíso, Chile

UNIVERSIDAD TECNICA
FEDERICO SANTA MARIA

Modeling and Control of Piezoelectric Actuators: An Irreversible port-Hamiltonian approach

Javier Alejandro Caballería Magna

Tesis de grado presentada como requisito parcial para optar al título de **Ingeniero Civil Electrónico** y al grado de **Magíster en Ciencias de la Ingeniería Electrónica**

Director de Tesis: Dr. Héctor Ramírez Estay

Defendida públicamente el 23 de noviembre de 2021 ante el jurado conformado por:

Dr. Juan I. Yuz	Universidad Técnica Federico Santa María
Dr. Héctor Ramírez	Universidad Técnica Federico Santa María
Dr. Alejandro Rojas	Universidad de Concepción
Dr. Yann Le Gorrec	FEMTO-ST Institute, University Bourgogne-Franche Comté

dedicado a mis padres: Margarita y Osvaldo

Acknowledgements

Esta tesis de magíster no fue fácil de realizar y no tengo dudas que sin la ayuda que recibí de las personas que estuvieron a mi lado durante este tiempo no creo que pudiera haber llegado tan lejos.

Primero me gustaría agradecer al director de esta tesis: al profesor Héctor Ramírez. Profesor, muchísimas gracias por estos casi tres años de trabajo juntos, por sus consejos, por ayudarme cuando estaba perdido en el vasto mundo de la ciencia, por animarme cuando más de una vez ya me estaba dando por vencido y por creer en mí. De verdad estoy muy agradecido y no puedo nada más que desearle lo mejor en esta vida.

Agradecer a mis compañeros de carrera que con el pasar de los años se convirtieron en amigos, Wala, Danas, Villa, Panchoso, Franco, Negro, Seba, Ignacio, gracias por los buenos momentos, risas, cervezas, estudios, etc. También agradecer a quienes son mis amistades más longevas de mi vida, Roxy, Vale, Meza, muchísimas gracias por su constante apoyo. Son todos ustedes unos tipos/as fantásticos, no les puedo desear nada más que la felicidad eterna.

También quiero agradecer a mis hermanos Andrea y Osvaldo, gracias por hacer de mi vida universitaria más fácil de llevar, por compartir su sabiduría y consejos conmigo. Finalmente pero no menos importante, agradecer a mis papás Osvaldo y Margarita, infinitas gracias por quererme y apoyarme, por el gran sacrificio que fue criar a tres hijos, proveerles una muy buena educación y que nunca nos faltara nada. Esta victoria no es solo mía, es de ustedes también.

Contents

1 Introduction **1**
1.1 Organization of the chapters of this thesis . . . 2
1.2 Main Contributions . . . 2

2 Models of Piezoelectric Actuators **4**
2.1 Dynamics Models with Hysteresis . . . 4
2.1.1 Linear Model . . . 5
2.1.2 Preisach Model . . . 5
2.1.3 Prandtl-Ishlinskii . . . 7
2.1.4 Bouc-Wen Model . . . 8
2.1.5 Maxwell Resistive Capacitor . . . 9
2.1.6 Hysteron . . . 10

3 IPHS Model of a class of piezoelectric actuator **14**
3.1 Port-Hamiltonian Systems . . . 14
3.1.1 The Mass-Spring-Damper System . . . 15
3.2 Irreversible Port-Hamiltonian Systems . . . 17
3.2.1 Example: Gas-Piston System . . . 18
3.2.2 IPHS formulation of a RLC circuit with hysteron . . . 20
3.3 The Piezoelectric Actuator as IPHS . . . 21
3.3.1 Mechanical Domain . . . 22
3.3.2 Electrical Domain . . . 22
3.3.3 Thermodynamic Domain . . . 23
3.3.4 IPHS Representation . . . 24
3.3.5 Numerical Simulations . . . 26

4 Control of the piezoelectric actuator **31**
4.1 Some preliminaries on stability . . . 31
4.2 Control design . . . 33
4.2.1 Characterization of equilibrium points . . . 33
4.2.2 Control design of the nominal system . . . 35
4.2.3 Control of the perturbed system . . . 36

5 Conclusions **38**

Bibliography **39**

Abstract

In a first part an irreversible port-Hamiltonian system formulation of a class of piezoelectric actuator with non-negligible entropy increase is proposed. The proposed model encompasses the hysteresis and the irreversible thermodynamic changes due to mechanical friction, electrical resistance and heat exchange between the actuator and the environment. The electro-mechanical dynamic of the actuator is modeled using a non-linear resistive-capacitive-inductor circuit coupled with a mass-spring-damper system, while the non-linear hysteresis is characterized using hysterons. The thermodynamic behavior of the model is constructed by making the electro-mechanical coupling temperature dependent, and by characterizing the entropy produced by the irreversible phenomena. By means of numerical simulations it is shown that the proposed model is capable of reproducing the expected behaviors and is in line with reported experimental results.

In a second part the proposed model is used to synthesize a non-linear passivity based controller for a class of piezoelectric actuator. The controller is designed starting from a nominal model which is obtained under the assumption that the electro-mechanical coupling is independent of the temperature. For this nominal model a control law which asymptotically stabilizes the closed-loop system at the desired dynamic equilibrium is proposed. In a second instance, the proposed model is obtained by perturbing the nominal model with the temperature dependent electro-mechanical coupling. Lyapunov perturbation theory is then used to show that under some general operation assumptions the proposed passivity based controller asymptotically stabilizes the closed-loop system. The control action can be interpreted in terms of damping/entropy injection with respect to the desired dynamic equilibrium.

Chapter 1

Introduction

Multi-physical systems are system whose dynamic behavior is generated by different physical phenomena. These systems encompass chemical processes, nano/micro-mechanical systems, smart materials, heat transfer processes, piezoelectric actuators, etc. Moreover, usually the approach to model multi-physical systems is by decomposing it into a set of more simple interconnected subsystems. Hence, using an appropriate framework, they can be studied and analyzed in a modular manner if the properties of its subsystems are understood [1].

The port-Hamiltonian framework has been effectively used to model multi-physical systems, specially electrical, mechanical, electro-mechanical systems [1, 2]. This theory is based on the first law of the thermodynamics, conservation of the internal energy, [2, 3] and provides a clear physical interpretation. Besides, a port-Hamiltonian system is composed by the interconnection of energy storing and energy dissipating elements, which define a set of matrices in addition to an Hamiltonian energy function determined by the parameters of the energy storing elements.

Thermodynamic systems deals with irreversible phenomena that can be caused by friction, heat transfer, electric resistance, inelastic deformation of solids and chemical reactions, among others. In any irreversible process the entropy, and thereby the second law of thermodynamics plays a major role. Port-Hamiltonian systems have been extended to incorporate simultaneously the first and second law of the thermodynamics, this kind of systems are denominated Irreversible port-Hamiltonian systems [4, 5].

Piezoelectric actuators are a non-linear, multi-physical systems that exhibit irreversible phenomena due to the inelastic deformation when a voltage or force is applied to them [6, 7, 8, 9]. In this thesis work an irreversible port-Hamiltonian system formulation of a class of piezoelectric actuator with non-negligible entropy increase is proposed. This model represents the hysteresis and the irreversible thermodynamic changes using an idealized element denominated hysteron [10, 11, 12], while the electro-mechanical dynamic of the actuator is modeled using a non-linear resistive-capacitive-inductor circuit coupled with a mass-spring-damper system.

Then, a first approach using the proposed model to design and synthesize a non-linear passivity based controller (PBC) [13, 2, 5] is presented. The controller is designed using the analysis of stability of perturbed systems [14], therefore we can divide the design into two steps: First a PBC for a simplified nominal system is synthesized under some general operation assumptions. Under this assumptions a controller which asymptotically stabilizes

the nominal system is derived using as candidate Lyapunov function an energy based availability function [15, 16, 17, 18]. The second step is to perform a perturbed system stability analysis on the proposed irreversible port-Hamiltonian model with the controller designed in the first step to show the asymptotic stability of the piezoelectric actuator.

This thesis is partially financed by Chilean FONDECYT 1191544 and CONICYT BASAL FB0008 projects.

1.1 Organization of the chapters of this thesis

This thesis is divided into five main chapters.

- ***Chapter 2:*** In this chapter we give the state of the art of mathematical/physical representations of the dynamics of piezoelectric actuators for control purposes.

  The hysteresis representation via hysteron plays a major role in the development of our proposed irreversible port-Hamiltonian model, and it is presented using a resistance-inductor as an example.

- ***Chapter 3:*** A brief reminder of port Hamiltonian systems (PHS) is given along with their main characteristics. The PHS model of a mass-spring-damper system is also shown as an example.

  The definition of an Irreversible port-Hamiltonian system is presented and its main properties are analyzed, as well as, differences with respect to the port-Hamiltonian systems. Two examples are shown, a gas-piston system and a RLC non-linear circuit that uses the hysteron component.

  The IPHS formulation of the piezoelectric actuator is developed. The proposed model is composed by an electro-mechanical system that is interconnected via a transducer element, the hysteresis behavior is characterized using hysterons components. Numerical simulations of the proposed model are performed.

- ***Chapter 4:*** In this chapter, some fundamental theorems on Lyapunov stability are presented. Then, a first approach for using the proposed model to synthesize a non-linear passivity based position controller for a class of piezoelectric actuator is developed. The design strategy is based on the analysis of perturbed systems stability.

- ***Chapter 5:*** Conclusions and comments on future work are given in this chapter.

1.2 Main Contributions

The main contributions of this thesis can be summarized in the following points:

- An irreversible port-Hamiltonian system formulation for a class of piezoelectric actuators has been proposed.

- The non-linear hysteresis has been characterized using a linear inductor connected with a non-linear resistance which together form a component called hysteron.

- A passivity based controller is designed for the proposed model using the analysis of perturbed systems stability.

Chapter 2

Models of Piezoelectric Actuators

Piezoelectric actuators are a non-linear, multi-physical systems that exhibit irreversible phenomena due to the inelastic deformation when a voltage or force is applied to them, this affects significantly the tracking accuracy applications, which is a subject of study for many researchers.

In this chapter we present different models that characterize the dynamic behavior of piezoelectric actuators, such as: Linear, Preisach, Prandtl-Ishlinskii, Bouc-Wen, Maxwell Resistive Capacitor and Hysteron. We focus our review in the Hysteron which is a passive approach to represent the hysteresis behavior via the interconnection of two types of physical elements, an energy storage element and a resistive element. Using this idea we propose a hysteron composed by a inductor connected in series with a resistance that allows to represent hysteresis curves in the electrical domain.

2.1 Dynamics Models with Hysteresis

Micro-manipulators, micro-grippers or micro-robots in general are widely used in micro-manipulation systems covering industrial manufacturing, pharmaceutics, biological and medical fields, and are of special importance in micro-assembly process. There are several reasons why micro-manipulators require special consideration. The first reason is that as the size of the involved parts lies in the millimetre or micron, the strength and stiffness compared to those of macro components is much smaller and thus micro-miniature parts are very easily damaged. Another important reason is that adhesion phenomena in micro-assembly process are a difficult problem that limits the development of micro-grippers. According to the driving force, micro-actuators can be divided into piezoelectric-ceramic-based, electrostatic-based, electromagnetic-force-based, electric-based, vacuum, adhesive-material-based, shape-memory-alloy-based, and so on [19].

Piezoelectric actuators, compared with other kinds of micro-actuators, are the most widely used ones because of their unique properties such as direct and reverse piezoelectric effects, their small size, high resolution, high bandwidth and high force density. This actuators are utilized to generate controllable displacement in micro/nano robotic applications [6, 20, 21, 22, 23]. It is well known that piezoelectric actuators exhibit hysteresis in their dynamics, which is due to irreversible thermodynamic phenomena. An important aspect

to consider in automatic control applications, such as position tracking or force control, is to compensate for the non-linear behavior caused by the hysteresis. This is a widely investigated subject and various models have been proposed for piezo actuators, as for instance: Preisach [24, 25, 26], Prandtl-Ishlinskii [6, 9], Bouc-Wen [8, 27], generalized Maxwell resistive-capacitive model [7] or models based on hysterons [10, 12]. Using models of the hysteresis its non-linear effects have been compensated using for instance the inverse model in cascade with an electro-mechanical actuator model [6, 9, 8, 27]. Other approach is to use sensors to measure and compensate the non-linear behavior, but the integration in nano/micro applications is complicated given how expensive and bulky sensing elements for these applications are [28].

The irreversible thermodynamic phenomena in piezoelectric actuators are mainly due to internal mechanical friction, inelastic deformations, electrical resistance and heat transfer with the surroundings. For certain applications the performance of the actuator is highly sensitive to temperature changes [29, 30, 31, 32], hence in addition to characterizing the hysteresis a thermodynamic model has to be considered to characterize the temperature of the actuator.

In the following sections we summarized different models in existing in the literature that can represent the behavior of the piezoelectric actuator.

2.1.1 Linear Model

The linear model characterizes the dynamics of the piezoelectric actuator as a linear representation, it is presented in [33] where the results are based on linear piezoelectricity in which all the coefficients are treated as constants, independent of the magnitude and frequency of applied mechanical forces and electrical field. The constitutive relationships of this model are

$$T_p = c^E_{pq} S_q - e_{kp} E_k \tag{2.1}$$

$$D_i = e^E_{iq} S_q - \varepsilon^S_{ik} E_k \tag{2.2}$$

$$U = \frac{1}{2} c^E_{pq} S_p S_q + \frac{1}{2} \varepsilon^S_{ij} E_i E_j \tag{2.3}$$

where T_p is the stress component, c_{pq} the elastic stiffness constant, S_q the strain component, $e.$ the piezoelectric constant, E_k the electric field component, D_i the electric displacement component, ε_{ij} the dielectric constants and U the stored energy density in the piezoelectric and finally $p, q = \{1, 2, 3, 4, 5, 6\}$ represents the space coordinates.

These equations state that the material strain and electrical displacement exhibited by a piezoelectric ceramic are both linearly affected by the mechanical stress and electrical field to which the ceramic is subjected [7].

This linear model does not to describe the non-linearities (hysteresis) that are inherent present in piezoelectric actuators.

2.1.2 Preisach Model

A classical Preisach model is used in [24, 25, 26] to identify the hysteresis behavior of the piezoelectric actuators. The equation that describes the hysteresis with this method is:

$$x(t) = \iint_{\alpha \geq \beta} \mu(\alpha, \beta) \gamma_{\alpha\beta}[u(t)] d\alpha d\beta \tag{2.4}$$

where $x(t)$ is the output displacement, $u(t)$ is the voltage input of the piezoelectric actuator, $\mu(\alpha, \beta)$ is a weighing function, commonly experimentally-obtained, in the Preisach model, α and β correspond to the threshold input values, $\gamma_{\alpha\beta}[u(t)]$ is known as a hysteresis operator or basic hysteron, whose value are zero or one, mathematically this can be written as follows, with $\beta \leq \alpha$:

$$\gamma_{\alpha\beta}[u(t)] = \begin{cases} 0 & u(t) \leq \beta \\ \gamma_{\alpha\beta}[u(t)] & \beta \leq u(t) \leq \alpha \\ 1 & u(t) \geq \alpha \end{cases} \tag{2.5}$$

and graphically Equation (2.5) is shown in Figure 2.1. Besides, to determining the weighting function $\mu(\alpha, \beta)$ in [24, 25, 26] they use the system's first-order reversal curves to construct a Everett function [26] as follows:

$$X(\alpha, \beta) = \frac{1}{2}(x_\alpha - x_{\alpha\beta}) \tag{2.6}$$

where x_α is defined as the piezoelectric expansion on the limiting ascending branch of the hysteresis curve corresponding to an input value α and, similarly $x_{\alpha\beta}$ is defined as the expansion on the descending branch that starts at the previous x_α, see Figure 2.2. This function will allow to avoid the double integration and finally obtain the following discrete Preisach model for the hysteresis, for more details see [26]:

$$x(t) = \begin{cases} X(u(t), \beta_N) + \sum_{i=1}^{N} (X(\alpha_i, \beta_{i-1}) - X(\alpha_i, \beta_i)) & \dot{u}(t) > 0 \\ X(\alpha_N, \beta_{N-1}) - X(\alpha_N, u(t)) + \sum_{i=1}^{N} (X(\alpha_i, \beta_{i-1}) - X(\alpha_i, \beta_i)) & \dot{u}(t) < 0 \end{cases} \tag{2.7}$$

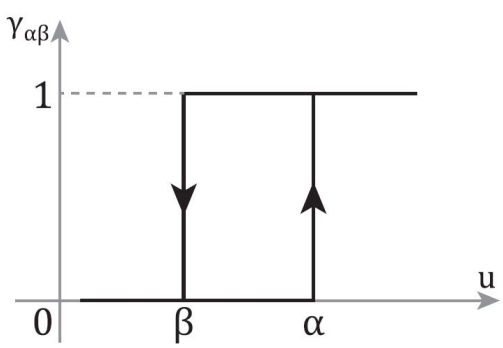

Figure 2.1: Basic hysteron with thresholds α, β. [26]

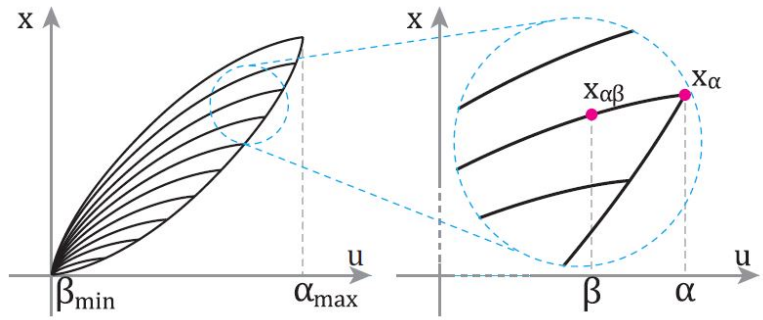

Figure 2.2: First-order reversal curves used to construct the Everett function. [26]

2.1.3 Prandtl-Ishlinskii

The Prandtl-Ishlinskii (PI) approach is commonly used to represent the hysteresis behavior of the piezoelectric actuators. To introduce this, the work [6] shows a lumped representation that models and control the position of a microgripper based on two piezocantilevers. This led to a non-linear model but they turn it to a linear one by compensating the hysteresis with its inverse, in order to achieve this objective they characterized the hysteresis by the Prandtl-Ishlinskii (PI) approach. Finally the model obtained is a transfer function, one-parameter dependent that links the control input and the output force of the piezocantilever.

Other approach to describe the dynamics of a bimorph piezoelectric cantilevered actuator is proposed in [9] where the dynamics are divided in two, a linear second order model of the actuator that is based on the Euler-Bernoulli beam theory and a non-linear hysteresis behavior that also is identified by the PI approach.

In the previous works, the common factor is that both used the Prandtl-Ishlinskii to characterize the hysteresis behavior and therefore calculate the inverse of the hysteresis to compensate this non-linearity behavior. The Prandtl-Ishlinskii approach is based on the weighted superposition of many elementary hysteresis operators also called play or backlash operator. This element is defined as follows:

$$\delta^{el}(t) = \max\left\{U(t) - r, \min\left\{U(t) + r, \delta^{el}(t - T)\right\}\right\} \tag{2.8}$$

where $U(t)$ is the input voltage signal, δ^{el} the output displacement of the operator, T is the sampling time and r the threshold of the operator, see Figure 2.3.

Thus, an hysteresis H_{st} is approximated by the sum of several play operators weighted by the gain (slope) w_i. Let n be a number of elements, so we have:

$$\delta(t) = H_{st}(U) = \sum_{i=1}^{n} w_i \max\left\{U(t) - r_i, \min\left\{U(t) + r_i, \delta_i^{el}(t - T)\right\}\right\} \tag{2.9}$$

with δ_i^{el} being the output of the ith play operator, r_i the threshold value of the ith operator and δ being the output of the actuator, for the piezoelectric case, the displacement. In

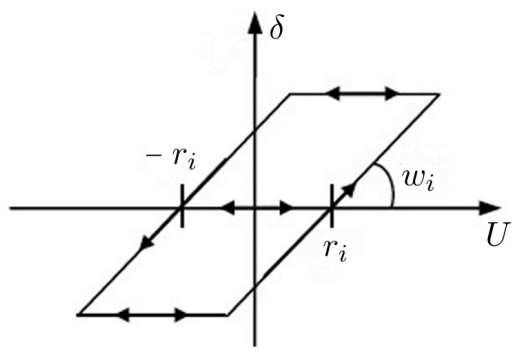

Figure 2.3: Curve of the i-th backlash opetaor.

Figure 2.3 we show the behavior of the i-th backlash operator.

Besides, the hysteresis inverse $H_{st}^{inv}(\cdot)$ is also a Prandtl-Ishlinskii model with r_i^{inv} thresholds and w_i^{inv} weightings. These parameters can be analytically computed using the parameters of the direct model [34, 6].

2.1.4 Bouc-Wen Model

Another way to represent the hysteresis effect of a piezoelectric actuator is by using the Bouc-Wen model [27] which allows to describe this behavior with compact equations, low numbers of parameters to identify will imply a easy implementation of this equations. The Bouc-Wen model is defined as a set of two differential equations that relates the applied mechanical f to the deformation x of the structure:

$$f(x, \dot{x}, h) = ak_0x + (1-\alpha)k_0h \tag{2.10}$$

$$\frac{dh}{dt} = \frac{dx}{dt}\left[A - |h|^m\left(\gamma + \beta \text{sgn}\left(\frac{dx}{dt}h\right)\right)\right] \tag{2.11}$$

where h represents an internal variable describing the structure inelastic behavior, k_0 and α denote the initial and the post-to-pre yield stiffness, respectively, and parameters A, β, γ controls the hysteresis shape and scale.

In [8] the model presented in Equations (2.10) and (2.11) is adapted to piezoelectric actuators. The resulting model is given by the following equations:

$$y(t) = d_pU(t) - h(t), \quad y(t_0) = y_0 \tag{2.12}$$

$$\frac{dh}{dt} = A\frac{dU}{dt} - \beta\left|\frac{dU}{dt}\right|h - \gamma\frac{dU}{dt}|h|, \quad h(t_0) = h_0 \tag{2.13}$$

where y is the displacement output, U is the applied voltage input, d_p is a parameter that represents the piezoelectric coefficient and is strictly positive.

The model described by Equations (2.12), (2.13) can be reduced if we write $h = H(U)$, where $H(U)$ is a non-linear operator characterized by the differential Equation (2.13):

$$y = d_p U - H(U) \tag{2.14}$$

this reduction is useful to use in a feedforward compensator of the hysteresis because there is no need to invert the model, in fact, the compensator is given by:

$$U = \frac{1}{d_p}(y_r + H(U)) \tag{2.15}$$

where y_r is a displacement reference output. Note that the only term to invert is d_p which is strictly positive as stated before.

2.1.5 Maxwell Resistive Capacitor

In [7] a non-linear lumped-parameter model of a piezoelectric stack actuator is presented where the purpose of this model is to establish a relationship between the electrical and mechanical domain of this piezoelectric. In Figure 2.4 a schematic representation of the model is shown

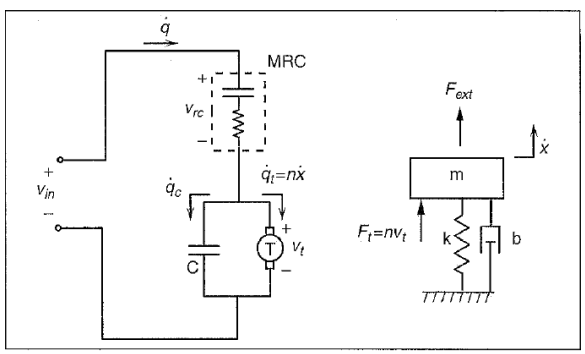

Figure 2.4: Physical system of a piezoelectric stack actuator. [7]

Thus, the model is represented by the interconnection of a mechanical mass-spring-damper system coupled with an non-linear electrical circuit and the hysteresis behavior is represented as a generalized Maxwell resistive capacitor (MRC in Figure 2.4) or Generalized Maxwell Slip. The different physical domains are interconnected by a transducer element T. Therefore, the behavior of the piezoelectric actuator is describe by the following set of equations

$$q = Tx + Cv_t \tag{2.16}$$

$$v_{in} = v_t + v_{rc} \tag{2.17}$$

$$v_{rc} = mrc(q) \tag{2.18}$$

$$F_t = Tv_t \tag{2.19}$$

$$m\ddot{x} + b\dot{x} + kx = F_t + f_{ext} \tag{2.20}$$

where q is the total charge in the ceramic, T is the electro-mechanical transducer ratio, x is the stack endpoint displacement, C is the linear capacitance in parallel with the transformer, v_t is the back-emf from the mechanical side, v_{in} is the actuator input voltage, v_{rc} is the voltage across the Maxwell capacitor (which is a function of q), F_t is the transduced force from the electrical domain, m, b and k are the mass, damping and stiffness of the ceramic, and f_{ext} is the force imposed from the external mechanical load.

The generalized Maxwell resistive capacitor is a component composed by the combination of a pure energy storage element coupled to a pure Coulomb friction element. The constitutive behaviour of the MRC is described by

$$V_i = \begin{cases} \dfrac{q - q_{b_i}}{C_i} & \text{if } \left| \dfrac{q - q_{b_i}}{C_i} \right| < v_i \\ v_i sgn(\dot{q}) \text{ and } q_{b_i} = q - C_i v_i sgn(\dot{q}) & \text{otherwise} \end{cases} \tag{2.21}$$

$$v_{rc} = \sum_{i=1}^{n} V_i \tag{2.22}$$

where V_i is the voltage output, C_i the capacitance, q_{b_i} the charge reference, and v_i the breakaway voltage of the $i-th$ resistive-capacitor element, v_{rc} is the voltage across the Maxwell capacitor. Note that the accuracy of the hysteresis depends on n resistive-capacitor elements which not affects to the order of the model but increases the computational calculations.

2.1.6 Hysteron

The hysteresis behavior can be modeled using a component called hysteron, that is presented in [10] and it consists of an energy consistent formulation. An hysteron is the interconnection of two basic physical elements, an energy storage element and a resistive element, both components are necessary because in the process of the hysteresis a part of the energy is dissipated and a part of the energy is conserved [11].

The constitutive equation of the energy storage element of the hysteron can be linear or non-linear and the resistive element is described by a non-linear equation. A peculiarity of the dissipating component is that has a dead zone and any curve must lay in first and third quadrant in order to satisfy the energy dissipation. A simple constitutive equation for the non-linear resistive element is given in Figure 2.5 for the electrical domain

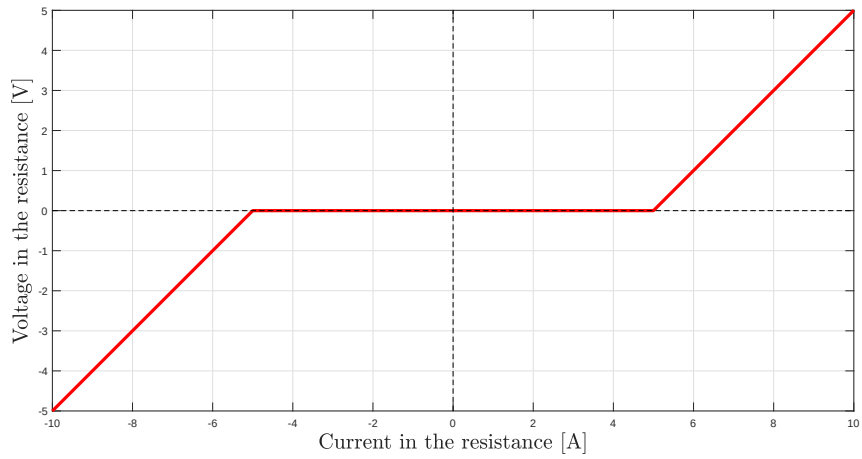

Figure 2.5: Non-linear relation between current and voltage

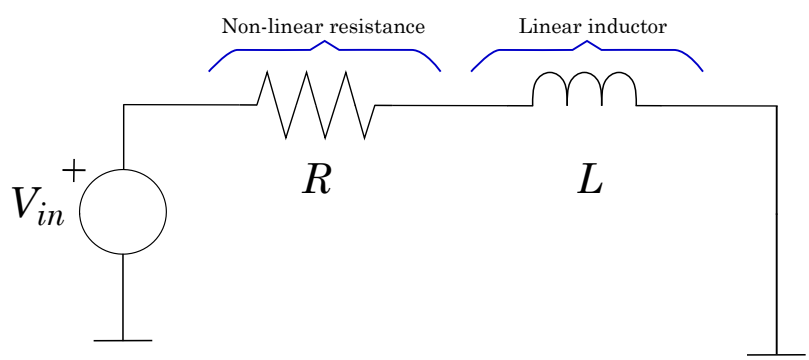

Figure 2.6: Diagram of one hysteron connected to a voltage input source

Let us consider, one hysteron as the combination of a non-linear resistance and a linear inductor in series, see Figure 2.6. Then, the Kirchhoff's voltage law gives us

$$V_{in} = V_R + V_L \tag{2.23}$$

where V_{in}, V_R and V_L are the voltage input, voltage of the resistance and voltage of the inductor respectively. Note that all the elements share the same current i.

The inductor is assumed to be linear with constitutive relation as

$$i = \frac{\phi}{L} \tag{2.24}$$

where ϕ is the magnetic flux of the inductor and L the inductance. The voltage of the resistance is defined as follows

$$V_R = w(i_R) \tag{2.25}$$

where i_R is the current through the resistance and $w(\cdot)$ is a non-linear operator that satisfies the properties of the Figure 2.5. Thus, $\dot{\phi}$ is equal to

$$\dot{\phi} = V_{in} - w\left(\frac{\phi}{L}\right) \tag{2.26}$$

Using this equations, a simulation is performed where the input is a sinusoidal wave, $V_{in} = 20\sin(2\pi t)$, and it is applied to only one hysteron. Figure 2.7 shows the hysteresis between voltage and magnetic flux for two different width of dead zone, $[-1, 1]$ and $[-5, 5][A]$ for the blue and red curve respectively.

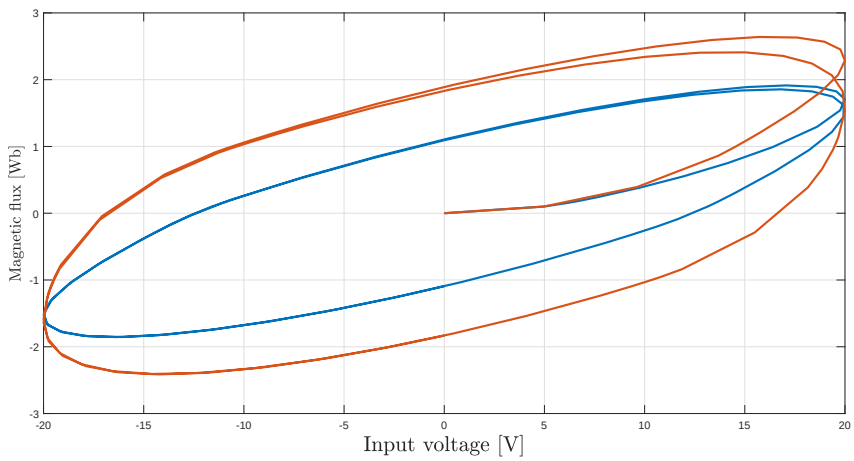

Figure 2.7: Simulation of one hysteron

In order to construct complex and more accurate hysteresis curves is necessary the interconnection of several hysterons [10]. For our particular case, this can be achieve by connecting the hysterons in parallel between them as in Figure 2.8.

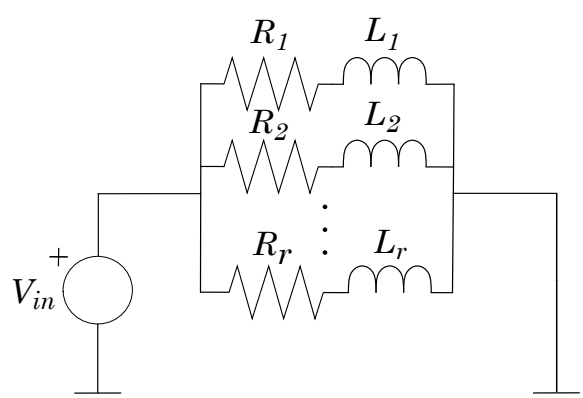

Figure 2.8: Diagram of r hysterons connected to a voltage input source

Then, the dynamic equation for each hysteron is

$$\dot{\phi}_j = V_{in} - w_j\left(\frac{\phi_j}{L_j}\right) \tag{2.27}$$

where ϕ_j is the magnetic flux of the $j-th$ inductor, L_j the inductance value of the $j-th$ inductor and $w_j(\cdot)$ the non-linear operator of the $j-th$ resistance. Thus, the current i is

$$i = \sum_{j=1}^{r} \frac{\phi_j}{L_j} \tag{2.28}$$

Note that the difference between the hysteron configuration presented in this thesis work with the equivalent electrical domain configuration presented in [10, 11], which consists in the interconnection of a capacitor with a resistance in series or parallel, not only relies in the energy storing element, also we are able to disengage the input V_{in} from the non-linear operator $w(\cdot)$ that defines the constitutive relation for the resistive element.

Chapter 3

IPHS Model of a class of piezoelectric actuator

In this chapter an Irreversible port-Hamiltonian formulation of a class of piezoelectric actuators that includes the hysteresis behavior is presented.

In the first section, the definition of a port-Hamiltonian system is introduced, along with its main characteristics and properties. The mass-spring-damper system is used as an example of this framework. Then, in the following section the definition of an Irreversible port-Hamiltonian system is presented and its main properties and differences are analyzed, with respect to the port-Hamiltonian systems. Two examples are shown, a gas-piston system and an RLC non-linear circuit that uses the hysteron component.

Finally, in the last section the IPHS formulation of the piezoelectric actuator is developed. The proposed model is composed by an electro-mechanical system that is interconnected via a transducer element, the hysteresis behavior is characterized using hysterons components. Numerical simulations of the proposed model are performed.

3.1 Port-Hamiltonian Systems

Port-Hamiltonian systems (PHS) are a framework that allows to describe a large class of mechanical-electrical systems and it is based on the principle of conservation of energy [1, 13, 35].

This framework formalizes the modelling of complex multi-domain physical models as the interconnection of energy storing elements with energy dissipating elements via basic physical interconnection laws and uses the total energy of the system, also denominated as Hamiltonian function, as the link between all the physical domains. This approach has been used in passivity-based control (PBC) techniques providing a clear physical interpretation of the control design problem [2, 3].

Definition 3.1 *Port-Hamiltonian systems are defined by the dynamic equations [13]:*

$$\dot{x} = [J(x) - R(x)]\frac{\partial H}{\partial x}(x) + g(x)u(t) \tag{3.1}$$

$$y = g^T(x)\frac{\partial H}{\partial x}(x) \tag{3.2}$$

where $x \in \mathbb{R}^n$ is the state variable, $u \in \mathbb{R}^m$ and $y \in \mathbb{R}^n$ are the input and output of the system respectively, $g(x) \in \mathbb{R}^{n\times m}$ is the input mapping to the system, $H(x) : \mathbb{R}^n \to \mathbb{R}$ is a function that represents the internal energy of the system and it is denominated as Hamiltonian, $J(x) = -J(x)^T \in \mathbb{R}^{n\times n}$ is a skew-symmetric matrix that represents the interconnection structure of the system, $R(x) = R(x)^T \geq 0 \in \mathbb{R}^{n\times n}$ is a symmetric matrix and corresponds to the resistive structures of the system. □

Furthermore the structure matrix $J(x)$ relates to a symplectic geometry as it defines a Poisson Bracket, if it satisfies the Jacobi identities [13]. The Poisson bracket of two functions $C^\infty(\mathbb{R}^n)$, Z and G is expressed as follows [36, 4].

$$\{Z, G\}_{J(x)} = \frac{\partial Z}{\partial x}^T J(x) \frac{\partial G}{\partial x} \tag{3.3}$$

The PHS dynamical equation, with dissipation matrix $R(x) = 0$, can be expressed in terms of the Poisson brackets as

$$\dot{x} = \{x, H\}_{J(x)} + g(x)u(t) \tag{3.4}$$

Port-Hamiltonian systems fulfill the first principle of the thermodynamics: conservation of the energy. Taking the following balance equation

$$\begin{aligned} \frac{dH}{dt} &= \frac{\partial H}{\partial x}^T \frac{dx}{dt} \\ &= \frac{\partial H}{\partial x}^T [J(x) - R(x)] \frac{\partial H}{\partial x}(x) + \frac{\partial H}{\partial x}^T g(x)u(t) \end{aligned}$$

Thus, by the skew-symmetry of $J(x)$, the balance equation of the internal energy is:

$$\frac{dH}{dt} = -\{H, H\}_{R(x)} + y^T u \tag{3.5}$$

where the first term of (3.5) represents the loss of the internal energy in the systems due to dissipative elements. Suppose that we have a lossless dissipative system, this means $R(x) = 0$, the balance Equation (3.5) is now:

$$\frac{dH}{dt} = y^T u \tag{3.6}$$

This equation represents that the internal energy will change with supply rate $y^T u$ and if we do not have any input to the system, Equation (3.6) is equal to zero, this means that the internal energy of the system is conserved.

3.1.1 The Mass-Spring-Damper System

As an illustrative example, consider the mass-spring-damper (MSD) system in Figure 3.1 and assume that the effects of friction between the mass and the surface is negligible

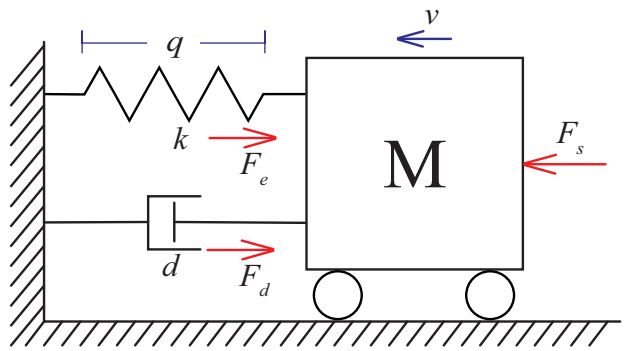

Figure 3.1: Mass-spring-damper system

where q is the relative displacement across the spring, v is the velocity of the mass, p represents the kinetic momentum, F_e, F_d and F_s are the elastic, damper and external force respectively, M is the mass, d is the damper constant and k is the Spring Hooke's law constant.

To obtain the port-Hamiltonian model of this system, first the interconnection relations for the forces and velocities are

$$\begin{aligned} F &= -kq - d\dot{q} + F_s \\ v_d &= v_m = \dot{q} \end{aligned}$$

where F represents the net force (mass times acceleration) when the system is on movement. Note that the spring and damper are assumed to be linear. Then, we obtain the state equations for the PHS model

$$\dot{q} = \frac{p}{M} \tag{3.7}$$

$$\dot{p} = -kq - d\frac{p}{M} + F_s \tag{3.8}$$

The mechanical energy is given by

$$H(q,p) = \frac{1}{2}kq^2 + \frac{1}{2}\frac{p^2}{M} \tag{3.9}$$

Finally, the port-Hamiltonian model of the MSD is:

$$\begin{aligned} \begin{bmatrix} \dot{p} \\ \dot{q} \end{bmatrix} &= \left(\begin{bmatrix} 0 & 1 \\ -1 & 0 \end{bmatrix} - \begin{bmatrix} 0 & 0 \\ 0 & d \end{bmatrix} \right) \begin{bmatrix} kq \\ \frac{p}{M} \end{bmatrix} + \begin{bmatrix} 0 \\ 1 \end{bmatrix} F_s \\ y &= \begin{bmatrix} 0 & 1 \end{bmatrix} \begin{bmatrix} kq \\ \frac{p}{M} \end{bmatrix} \end{aligned} \tag{3.10}$$

with constant matrices J, R satisfying $J = -J^T$ and $R = R^T \geq 0$.

3.2 Irreversible Port-Hamiltonian Systems

The irreversible port-Hamiltonian system (IPHS) [4, 5] are an extension of PHS that encompasses the first and second principle of thermodynamics, that is the conservation of the internal energy and irreversible entropy creation, as structural properties. The definition of IPHS not only allows to represent the irreversible phenomena of the system, also includes the reversible phenomena.

Definition 3.2 *An Irreversible Port-Hamiltonian System (IPHS) is defined by the dynamic equation [12, 5]:*

$$\dot{x} = J_{ir}\left(x, \frac{\partial U}{\partial x}\right)\frac{\partial U}{\partial x}(x) + g\left(x, \frac{\partial U}{\partial x}\right)u(t) \tag{3.11}$$

$$y = g\left(x, \frac{\partial U}{\partial x}\right)^T \frac{\partial U}{\partial x}(x) \tag{3.12}$$

where $x \in \mathbb{R}^n$ is the state variable, $U : C^\infty(\mathbb{R}^n) \to \mathbb{R}$ is the Hamiltonian function, $S : C^\infty(\mathbb{R}^n) \to \mathbb{R}$ represents the entropy, the matrix J_{ir} is skew-symmetric and is defined as:

$$J_{ir}\left(x, \frac{\partial U}{\partial x}\right) = J_0(x) + R\left(x, \frac{\partial U}{\partial x}\right)J \tag{3.13}$$

where $J_0(x)$ is the structure matrix of a Poisson bracket and $S(x)$ is a Casimir function of $J_0(x)$, $J = -J^T \in \mathbb{R}^{n\times n}$ is a constant skew-symmetric matrix, $R\left(x, \frac{\partial U}{\partial x}\right)$ is the product of a positive definite function γ and the Poisson bracket of the entropy S and the Hamiltonian U defined as:

$$R = R\left(x, \frac{\partial U}{\partial x}\right) = \gamma\left(x, \frac{\partial U}{\partial x}\right)\{S, U\}_J \tag{3.14}$$

with $\gamma\left(x, \frac{\partial U}{\partial x}\right) \geq 0$ a non-linear positive function of the states and co-states that might be only a function of the states. Also, $u \in \mathbb{R}^m$ is the external input to the system and $g\left(x, \frac{\partial U}{\partial x}\right) \in \mathbb{R}^{n\times m}$ is the input mapping to the system. □

Let us derive from the balance equations of the total energy function $U(x)$ and entropy function $S(x)$ the two principles of thermodynamics. Taking the derivative of $U(x)$ respect to time

$$\frac{dU}{dt} = \{U, U\}_{J_0(x)} + R\{U, U\}_J + y^T u$$

by the skew-symmetry property of J and J_0, the Poisson brackets $\{U, U\}_J$, $\{U, U\}_{J_0}$ are equal to zero, this led us to:

$$\frac{dU}{dt} = y^T u$$

the previous equation represents that the system defined in (3.11)-(3.12) is a lossless dissipative system with energy supply rate $y^T u$, this means that the variation of energy is due to

its interaction with the environment, hence satisfies the first principle of thermodynamics. Now taking the balance equation of the entropy function gives us

$$\frac{dS}{dt} = \{S, U\}_{J_0(x)} + R\{S, U\}_J + y_s^T u$$

where $y_s = \frac{\partial S}{\partial x}^T(x)g$ is an entropy conjugated output. The term $\{S, U\}_{J_0(x)} = 0$ for any Hamiltonian $U(x)$ because $J_0(x)$ is a Casimir function of $S(x)$. In the absence of some internal input, i.e., $u = 0$, and by the definition of the modulating function (3.14) we obtain

$$\frac{dS}{dt} = \gamma\left(x, \frac{\partial U}{\partial x}\right)\{S, U\}_J^2 = \sigma_s(x) \geq 0 \tag{3.15}$$

where $\sigma_s(x)$ is the internal entropy production, this expresses that for a thermodynamic system the variation of the entropy function is greater or equal to zero and equal to $\sigma_s(x)$, in accordance with the second principle of the thermodynamics.

The difference between the PHS definition and the IPHS relies in the modulating function R that depends of the co-states destroying the linearity of any Poisson tensor [5]. Besides the Poisson bracket $\{S, U\}_J$ defines the thermodynamic driving force of the system [4].

3.2.1 Example: Gas-Piston System

Consider a gas contained in a cylinder closed by a piston submitted to gravity [5], the objective is to obtain the irreversible port-Hamiltonian system. To achieve this, we can divide the dynamics of this system as two, the effect of the piston under the gravitation field and the properties of the perfect gas. The first is determined by the sum of the kinetic and potential energy, the second may be defined by its internal energy, for this example is supposed that there is no exchange of matter. The total energy of the system is

$$E(x) = H_{mec}(z, p) + U(S, V)$$

where z is the altitude of the piston, p the kinetic momentum, $U(S, V)$ represents the internal energy, S is the entropy variable, V is the volume variable and x is the state vector given by $x = [S, V, z, p]^T$. Note that N represents the number of moles and it is a constant for this example and $H_{mec}(z, p)$ is defined as follows

$$H_{mec}(z, p) = \frac{1}{2}mp^2 + mgz \tag{3.16}$$

where m is the piston mass. The co-energy vector and variables are defined by the gradient of the total energy $E(x)$, this is:

$$\begin{aligned}
\frac{\partial E}{\partial S} &= T \\
\frac{\partial E}{\partial V} &= -P \\
\frac{\partial E}{\partial z} &= mg = F_g \\
\frac{\partial E}{\partial p} &= v
\end{aligned}$$

where T is the temperature, P is the pressure, F_g is the gravity force and v is the velocity of the piston.

The gas in the cylinder under the piston may undergo a non-reversible transformation when the piston moves. We assume that in this case a non-adiabatic transformation due to mechanical friction (and/or viscocity of the gas), and that the dissipated mechanical energy is converted entirely into heat flow in the gas. The resisting mechanical force due to friction is $F_r = v\nu$. Then, the entropy balance equation is

$$\frac{dS}{dt} = \frac{1}{T}\nu v^2 = \sigma_{int} \tag{3.17}$$

which is the irreversible entropy flow at temperature T, induced by the heat flow νv^2 due to the friction of the piston. In the following equation is shown the coupling between the piston and the gas

$$\begin{bmatrix} f_V^e \\ F^e \end{bmatrix} = \begin{bmatrix} 0 & A \\ -A & 0 \end{bmatrix} \begin{bmatrix} -P \\ v \end{bmatrix}$$

where f_V^e is the variation of the volume of the gas, F^e is the relating force, A is the area of the piston.

The dynamics of the gas-piston system is given by the following set of equations

$$\begin{aligned} \frac{dS}{dt} &= \frac{1}{T}\nu v^2 \\ \frac{dV}{dt} &= Av \\ \frac{dz}{dt} &= v \\ \frac{dp}{dt} &= -F_g + AP - F_r = -mg + AP - \nu v \end{aligned} \tag{3.18}$$

The first equation is the entropy balance accounting for the irreversible creation of entropy due to the mechanical friction. The second equation indicates that the motion of the piston induces a variation of the volume of the gas. The third euqation defines the velocity of the piston. The last equation is the Newton's law applied to the piston. This control system can be written in state space representation form as follows:

$$\frac{d}{dt}\begin{bmatrix} S \\ V \\ z \\ p \end{bmatrix} = \begin{bmatrix} 0 & 0 & 0 & \frac{\nu v}{T} \\ 0 & 0 & 0 & A \\ 0 & 0 & 0 & 1 \\ -\frac{\nu v}{T} & -A & -1 & 0 \end{bmatrix} \begin{bmatrix} T \\ -P \\ F \\ v \end{bmatrix}$$

Thus, it can be identified the IPHS structure matrix $J_{ir}(T, v)$ and its decomposition from definition 3.2:

$$J_{ir}(T, v) = J_0 + R\left(x, \frac{\partial U}{\partial x}\right) J$$

where the constant Poisson structure matrix is:

$$J_0 = \begin{bmatrix} 0 & 0 & 0 & 0 \\ 0 & 0 & 0 & A \\ 0 & 0 & 0 & 1 \\ 0 & -A & -1 & 0 \end{bmatrix} \tag{3.19}$$

and the matrix associated to the irreversible phenomena is:

$$R\left(x, \frac{\partial U}{\partial x}\right) J = \frac{\nu v}{T} \begin{bmatrix} 0 & 0 & 0 & 1 \\ 0 & 0 & 0 & 0 \\ 0 & 0 & 0 & 0 \\ -1 & 0 & 0 & 0 \end{bmatrix} \tag{3.20}$$

3.2.2 IPHS formulation of a RLC circuit with hysteron

As illustrative example, consider the RLC circuit of the Figure 3.2, which is conformed by a voltage input source V_{in}, one hysteron defined as in Section 2.1.6 and a linear capacitor. The objective is to obtain an IPHS formulation for this system

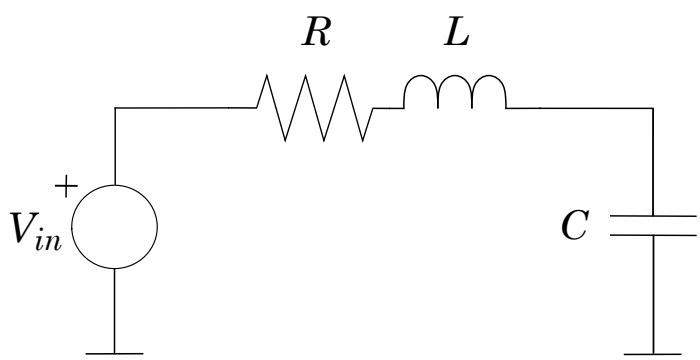

Figure 3.2: RLC circuit diagram

The state equations that characterize this system are

$$\dot{Q} = \frac{\phi}{L} \tag{3.21}$$

$$\dot{\phi} = V_{in} - \frac{Q}{C} - w\left(\frac{\phi}{L}\right) \tag{3.22}$$

where Q is the charge in the capacitor, ϕ is the electromagnetic flux of the inductor, C and L are the capacitance and inductance respectively. Besides, as it was defined in Section 2.1.6 one hysteron is the interconnection between the non-linear resistance with a linear inductor in series. The resistance has the following constitutive law

$$V_R = w(i_R)$$

where $w(\cdot)$ is a non-linear, non-smooth operator that must satisfy the following dissipation relation

$$V_R i_R = w(i_R) i_R \geq 0 \tag{3.23}$$

The internal energy of the system, which is the sum of the electrical energy and a smooth function of the entropy

$$U = \frac{1}{2}\frac{Q^2}{C} + \frac{1}{2}\frac{\phi^2}{L} + f(S) \tag{3.24}$$

the variation in time of the internal energy is given by

$$\dot{U} = -\frac{\phi}{L} w\left(\frac{\phi}{L}\right) + V_{in}\frac{\phi}{L} + \frac{\partial U}{\partial S}\dot{S}$$

From Gibb's relation [37] we have that $\frac{\partial U}{\partial S} = T(S)$. Now suppose that there is not input, i.e. $V_{in} = 0$, then it is obtained

$$\dot{S} = \frac{1}{T}\frac{\phi}{L} w\left(\frac{\phi}{L}\right) = \sigma \geq 0 \tag{3.25}$$

where σ corresponds to the internal entropy production and it is related to the electrical dissipation of the hysteron. The IPHS formulation of the RLC hysteron circuit is then

$$\begin{bmatrix} \dot{Q} \\ \dot{\phi} \\ \dot{S} \end{bmatrix} = \left(\begin{bmatrix} 0 & 1 & 0 \\ -1 & 0 & 0 \\ 0 & 0 & 0 \end{bmatrix} + \frac{1}{T} w\left(\frac{\phi}{L}\right) \begin{bmatrix} 0 & 0 & 0 \\ 0 & 0 & -1 \\ 0 & 1 & 0 \end{bmatrix} \right) \begin{bmatrix} \frac{Q}{C} \\ \frac{\phi}{L} \\ T \end{bmatrix} + \begin{bmatrix} 0 \\ 1 \\ 0 \end{bmatrix} V_{in} \tag{3.26}$$

Note that this example shows the main reason to use hysterons to represent the hysteresis, which is a passive approach, allowing incorporate the hysteresis as by an energy preserving interconnection with the rest of the system [10, 12].

3.3 The Piezoelectric Actuator as IPHS

In this section we develop an IPHS formulation for the proposed model shown in Figure 3.3 that represents the electro-mechanical part of the piezoelectric actuator.

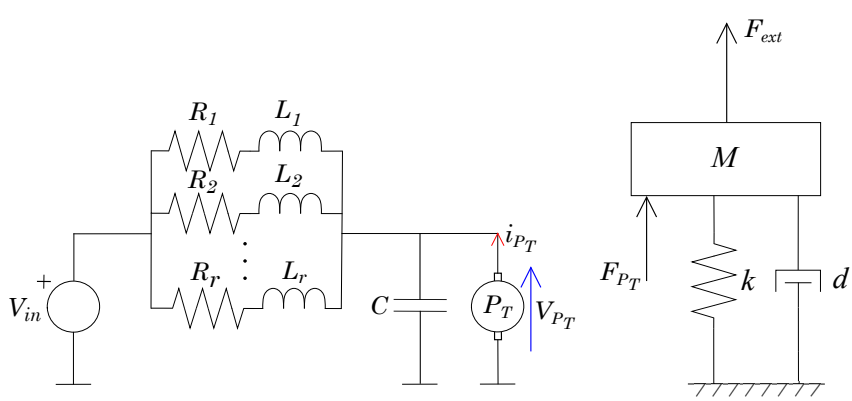

Figure 3.3: Piezoelectric actuator model

This model is based on the work of Goldfarb and Celanovic [7], where a lumped-parameter model of a piezoelectric stack actuator is represented by an electrical subsystem with a nonlinear hysteresis element and a mechanical subsystem. The electrical and mechanical domains are coupled through a transducer element P_T. Different to the model in [7], we model the hysteresis by the interconnection of hysterons [10, 12]. In the following subsections we present the model of each physical subdomain of before giving the complete thermo-electro-mechanical model the piezo actuator.

3.3.1 Mechanical Domain

The mechanical part of the piezoelectric actuator is represented by a mass-spring-damper system with parameters M, k and d respectively. The interconnection relations for the forces and velocities are

$$\begin{aligned} F_M &= -F_k - F_d + F_{P_T} + F_{ext} \\ v_M &= v_d = \dot{q} \end{aligned}$$

where F_M is the force over the mass, F_k is the elastic force from the spring, F_d is the damping force, F_{ext} is an external force and F_{P_T} is the force produced by electro-mechanical coupling, v_M and v_s are the velocities of the damper and the mass respectively and q is the tip displacement of the piezoelectric actuator. The spring and damper are assumed to be linear. Thus, the constitutive laws of the energy storage elements can be expressed as

$$F_e = k(q - q_l), \quad F_d = dv_d, \quad v_M = \frac{p}{M}$$

where q_l is the displacement of the spring in rest position and p the kinetic momentum. Taking as state variables the pair (q, p) the dynamic equations of this subsystem are

$$\begin{aligned} \dot{q} &= \frac{p}{M} \\ \dot{p} &= -k(q - q_l) - d\frac{p}{M} + F_{P_T} + F_{ext} \end{aligned}$$

3.3.2 Electrical Domain

The electrical part of the piezoelectric model is composed by a voltage source, which is the input of the system, a capacitor of capacitance C and r hysterons, each composed by a resistance and an inductor in series. The interconnection relations are

$$\begin{aligned} V_{R_j} + V_{L_j} + V_C &= V_{in} \\ V_{R_j} + V_{L_j} &= V_{R_k} + V_{L_k} \text{ for } j \neq k \\ i_C &= \sum_{j=1}^{r} i_{h_j} - i_{P_T} \end{aligned}$$

where $j, k = \{1, 2, \cdots, r\}$; V_{R_j}, V_{L_j} and V_C are the voltage of the j-th resistance, j-th inductor and capacitor respectively; i_C, i_{h_j} and i_{P_T} are the currents through the capacitor, j-th hysteron and the transducer respectively. The constitutive laws for the energy storage elements are considered linear,

$$i_{L_j} = \frac{\phi_j}{L_j}, \quad V_C = \frac{Q}{C}$$

where i_{L_j} is the current through the j-th inductor, ϕ_j the electromagnetic flux of the j-th inductor, Q is the charge stored in the capacitor, L_j is the inductance of the j-th inductor and C is the capacitance. The r resistances are non-linear with constitutive law $V_{R_j} = w_j(i_{R_j}, T)$ where $w_j(\cdot, T)$ is a non-linear, non-smooth operator satisfying the dissipation relation

$$V_{R_j} i_{R_j} = w_j(i_{R_j}, T) i_{R_j} = \sigma_{h_j} \geq 0 \tag{3.27}$$

where σ_{h_j} corresponds to the internal entropy production of the j-th hysteron. From the interconnection equations the following set of state equations are obtained

$$\dot{Q} = \sum_{j=1}^{r} \frac{\phi_j}{L_j} - i_{P_T}$$
$$\dot{\phi}_j = V_{in} - \frac{Q}{C} - w_{T_j}\left(\tfrac{\phi_j}{L_j}, T\right)$$

3.3.3 Thermodynamic Domain

We consider that the piezoelectric actuator is a thermodynamic system which exchanges heat with its environment. Denoting by S the total entropy of the system, the entropy balance is given by $\dot{S} = \sigma + \dot{S}_{en}$ where σ represents the internal entropy production and $\dot{S}_{en}$ the entropy exchanges with the environment which is modeled as

$$\dot{S}_{en} = \lambda \left(\frac{T_e(t)}{T(S)} - 1 \right) \tag{3.28}$$

where λ denotes the Fourier's heat conduction coefficient and $T_e(t)$ is the temperature of the environment. The constitutive relation considered for the temperature is

$$T(S) = T_0 e^{\frac{S}{c_0}} \tag{3.29}$$

where T_0 and c_0 are constants [5]. To obtain σ we consider the total energy function of the interconnected system

$$U = \frac{1}{2}k(q - q_l)^2 + \frac{1}{2}\frac{p^2}{M} + \frac{1}{2}\frac{Q^2}{C} + \frac{1}{2}\sum_{j=1}^{r} \frac{\phi_j^2}{L_j} + f_h(S) \tag{3.30}$$

where $f_h(S)$ is some smooth function of the entropy which is yet to be deduced. Assuming that there are no external inputs, i.e., $F_{ext} = 0$, $V_{in} = 0$, and $T_e = T$, which implies $\dot{S}_{en} = 0$,

the time variation of (3.30) is

$$\dot{U} = -\sum_{j=1}^{r} \frac{\phi_j}{L_j} w_j \left(\tfrac{\phi_j}{L_j}, T\right) - d\left(\frac{p}{M}\right)^2 + \frac{\partial U}{\partial S}\dot{S}$$

from were we obtain

$$\begin{aligned} \sigma &= \frac{1}{T}\left(\sum_{j=1}^{r} \frac{\phi_j}{L_j} w_j \left(\tfrac{\phi_j}{L_j}, T\right) + d\left(\frac{p}{M}\right)^2\right) \\ &= \sum_{j=1}^{r} \sigma_{h_j} + \sigma_d \geq 0 \end{aligned} \tag{3.31}$$

where σ_{h_j} and σ_d correspond respectively to the internal entropy production of the j-th hysteron and the damper. The entropy balance is given by

$$\dot{S} = \sum_{j=1}^{r} \sigma_{h_j} + \sigma_d + \lambda\left(\frac{T_e(t)}{T(S)} - 1\right)$$

3.3.4 IPHS Representation

In order to define the coupling relation between the thermal-electrical-mechanical we assume the following.

Assumption 3.1 *The three domains are interconnected through the hysterons by the non-linear resistances and by the transducer element P_T as follows*

$$V_{R_j} = w_j(i_{R_j}, T)$$

where $w_j(i_{R_j}, T)$ is an operator that depends on the temperature T but it is applied to the current i_{R_j}. Furthermore the transducer is temperature modulated, and defined by the following power preserving relations

$$F_{P_T} = \alpha(T)V_{P_T} = \alpha(T)V_C, \quad i_{P_T} = \alpha(T)v_{P_T} = \alpha(T)v_M$$

where α is the electro-mechanical transducer ratio which depends on the temperature T of the piezoelectric actuator.

Assumption 3.2 *The electro-mechanical transducer ratio is a linear function of the temperature, that is*

$$\alpha(T) = a_T T \tag{3.32}$$

where a_T is a constant.

Using Assumption 3.1 together with the balance equations deduced in the previous subsections,

$$\dot{q} = \frac{p}{M} \tag{3.33}$$

$$\dot{p} = -k(q - q_l) - d\frac{p}{M} + \alpha(T)\frac{Q}{C} + F_{ext} \tag{3.34}$$

$$\dot{Q} = \sum_{j=1}^{r} \frac{\phi_j}{L_j} - \alpha(T)\frac{p}{M} \tag{3.35}$$

$$\dot{\phi}_{L_j} = V_{in} - \frac{Q}{C} - w_j\left(\frac{\phi_j}{L_j}, T\right) \tag{3.36}$$

$$\dot{S} = \sum_{j=1}^{r} \sigma_{h_j} + \sigma_d + \lambda\left(\frac{T_e}{T} - 1\right) \tag{3.37}$$

the piezo actuator model allows the IPHS formulation given in the following proposition.

Proposition 3.1 *Consider $x = (q, p, Q, ., \phi_j, ., S)$ as state vector. Then a IPHS formulation for the thermo-electro-mechanical model of the piezo actuator characterized by (3.33)-(3.37) is*

$$\dot{x} = \left(J_0 + R_d J_d + \sum_{j=1}^{r} R_j J_j\right)\frac{\partial U}{\partial x} + gu \tag{3.38}$$

where the structure matrices are defined as

$$J_0 = \begin{bmatrix} 0 & 1 & 0 & 0 & \cdots & 0 & 0 \\ -1 & 0 & \alpha(T) & 0 & \cdots & 0 & 0 \\ 0 & -\alpha(T) & 0 & 1 & \cdots & 1 & 0 \\ 0 & 0 & -1 & 0 & \cdots & 0 & 0 \\ \vdots & \vdots & \vdots & \vdots & \ddots & \vdots & \vdots \\ 0 & 0 & -1 & 0 & \cdots & 0 & 0 \\ 0 & 0 & 0 & 0 & \cdots & 0 & 0 \end{bmatrix}, \tag{3.39}$$

J_d and J_j are have all their elements equal to zero except for two elements in each matrix, respectively

$$J_{d_{(n,2)}} = 1 \quad J_{d_{(2,n)}} = -1$$
$$J_{j_{(n,j+3)}} = 1 \quad J_{j_{(j+3,n)}} = -1$$

The non-linear modulating functions are

$$R_d = \frac{1}{T}d\left(\frac{p}{M}\right) \qquad R_j = \frac{1}{T}w_j\left(\frac{\phi_j}{L_j}, T\right)$$

The input vector is $u^T = (F_{ext}, V_{in}, \lambda\left(\frac{T_e}{T} - 1\right))$, with input mapping

$$g^T = \begin{bmatrix} 0 & 1 & 0 & 0 & \cdots & 0 & 0 \\ 0 & 0 & 0 & 1 & \cdots & 1 & 0 \\ 0 & 0 & 0 & 0 & \cdots & 0 & 1 \end{bmatrix}$$

and conjugated output $y^T = (\frac{p}{M}, \sum_{j=1}^{r} \frac{\phi_j}{L_j}, T)$.

From the proposed model the matrices J_d and J_k represent the interconnection of the dissipative elements (damper and hysterons) and J_0 represents the interconnection of the energy preserving elements. Note that J_0 depends on T which is a co-energy variable, implying it is a pseudo port-Hamiltonian matrix [38, 39].

In addition, the thermodynamic driving forces, associated with the damper and $j-th$ hysteron are, respectively, $\{S,U\}_{J_d} = \frac{p}{M}$ and $\{S,U\}_{J_j} = \frac{\phi_j}{L_j}$ while the positive definite modulation functions are $\gamma_d = \frac{d}{T}$ and $\gamma_j = \frac{1}{T}w_j(\cdot,T)$.

3.3.5 Numerical Simulations

In this subsection, numerical simulations are performed to verify that the proposed thermodynamic model reproduces the behavior of a piezoelectric actuator when the environment temperature and the frequency of the voltage input vary. Numerical values within standard physical ranges were considered for the electro-mechanical components [7, 40] while suitable values were selected for the thermodynamic parameters. The considered parameters are resumed in Table 3.1. No external mechanical loading has been considered, i.e., $F_{ext} = 0$.

M	k	d	C
$3,5 \cdot 10^{-3}[kg]$	$5 \cdot 10^5[N/m]$	$4 \cdot 10^2[N \cdot s/m]$	$5[\mu F]$
L	T_0	λ	c_0
$1 \cdot 10^{-3}[H]$	$296,15[K]$	$2[W/m^2K]$	$5[K/J]$

Table 3.1: Parameters of the model

Temperature dependent coupling elements

The electro-mechanical transducer ratio α, which is by assumption temperature dependent, is defined as

$$\alpha(T) = a\frac{T}{T_0}$$

where $a = 10$ with units $[C/m]$ or $[C/s \cdot kg]$ if it is the electrical to mechanical transducer ratio or mechanical to electrical, respectively. For simplicity two hysterons are used for the simulations. Notice that this is a very low number, and that to achieve complex and more precisely hysteresis curves a larger number of hysterons needs to be employed [10]. The inductance values are chosen equal for both hysterons and the non-linear resistance operators $w_j(z,T)$ defined as

$$w_j = \begin{cases} \frac{10}{T-T_0}(z-0.5) & z > 0.5 \\ 0 & -0.5 \leq z \leq 0.5 \\ \frac{10}{T-T_0}(z+0.5) & z < -0.5 \end{cases}$$

Notice that for this particular choice the reference temperature T_0 has to be selected lower than the operation range of T. Figure 3.4. shows the curve generated by the chosen non-linear operator for different values of T.

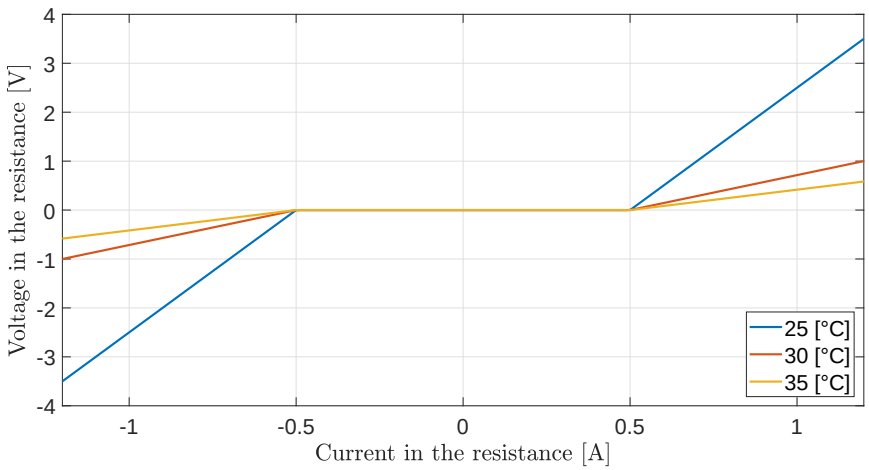

Figure 3.4: $w_j(\cdot, T)$ operator behavior for different temperatures values

Simulations Results

The hysteresis behavior is shown in Figure 3.5. A $100[V]$ sinusoidal input voltage at frequency $100[Hz]$ has been considered, i.e., $V_{in} = 100\sin(100 \cdot 2\pi t)[V]$, and different values for the external temperature $T_e = \{25, 30, 35, 40\}[°C]$ have been used. It is appreciated that the slope of the hysteresis curve changes when the external temperature changes. This is in accordance with reported results on temperature dependent hysteresis in piezoelectric actuators [31, 32] (see Figure 3.6).

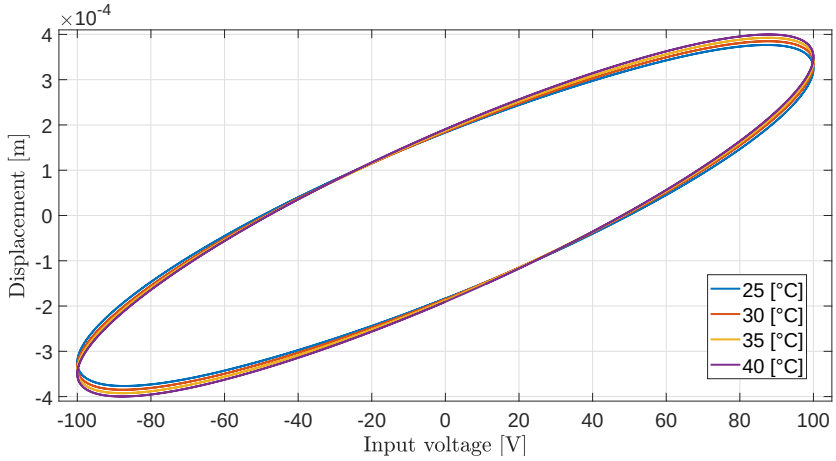

Figure 3.5: Hysteresis behavior between voltage and displacement under different environment temperatures

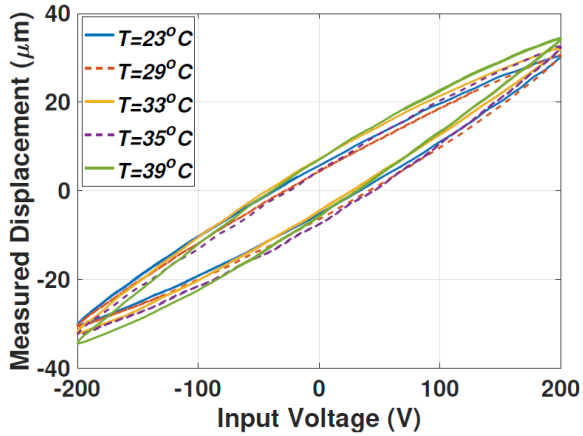

Figure 3.6: Hysteresis behavior presented by Al Janaideh et al., 2019 [32]

Figure 3.7 shows static temperature changes when the input voltage frequency f is increased, i.e., $V_{in} = 100\sin(f \cdot 2\pi t)[V]$, for different values of inductance in the hysterons, $L = \{0.1, 0.5, 1, 5, \} \cdot 10^{-3}[H]$. From the reported characteristics of commercial piezoelectric actuators, like the bimorph PB4NB2W from Thorlabs [40] (see Figure 3.8), it is expected that the static temperature of the actuator increases as the operation frequency increases. It is observed in Figure 3.7 that the aforementioned characteristic is achieved for a range of lower frequencies which depend on the value of the parameter L.

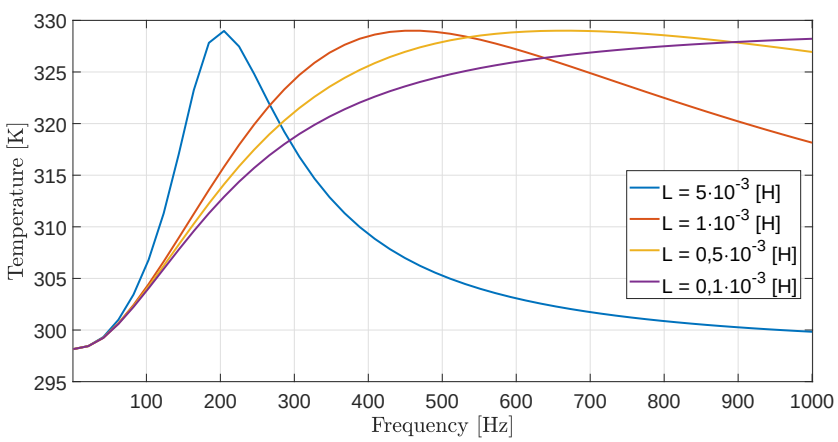

Figure 3.7: Static temperature change for different frequency operation

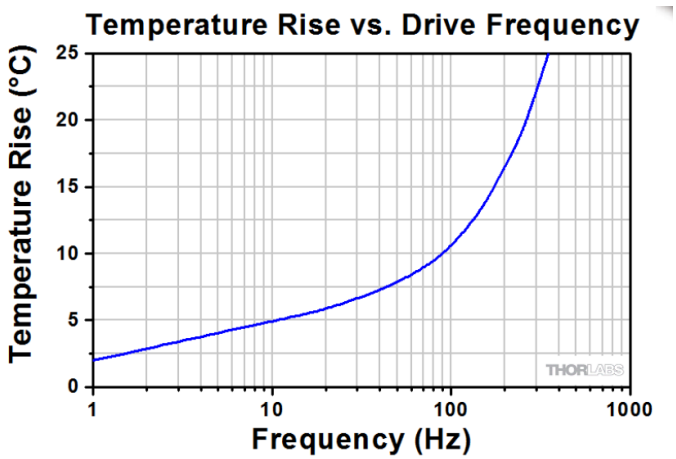

Figure 3.8: Change of temperature with respect to the frequency for a bimorph PB4NB2W Thorlabs, 2020 [40]

Figure 3.9 shows the displacement step response when the input voltage is changed from $50[V]$ to $100[V]$ for different external temperature values, $T_e = \{25, 30, 35, 40\}[C]$. The results show that the temperature generates an offset in the static response of the displacement, which is in accordance with reported results [31].

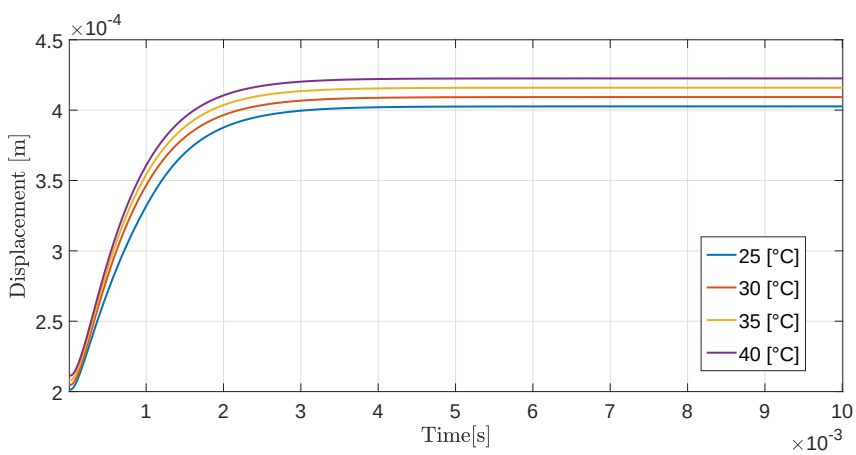

Figure 3.9: Step response for different environment temperatures

Figure 3.10 shows how the hysteresis curve changes for different voltage frequencies. In this simulation $V_{in} = 100\sin(f \cdot 2\pi t)[V]$ and $f = \{10, 50, 100, 200\}[Hz]$. Notice that the hysteresis curve gets wider and the slope decreases when the frequency is increases, as expected from reported results in [41, 42] (see Figure 3.11). These effects are a combination of the ones depicted in Figures 3.5 and 3.7.

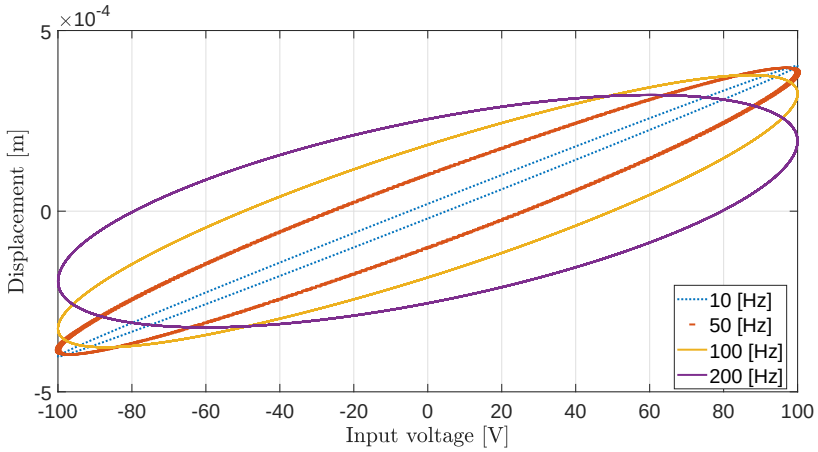

Figure 3.10: Change of the hysteresis curve due to the frequency operation

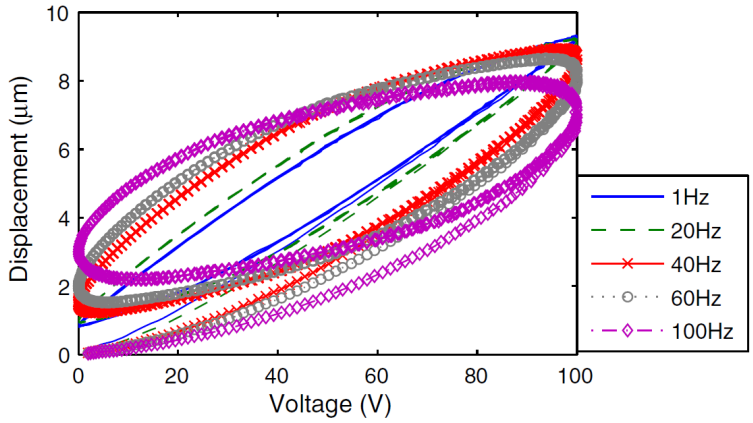

Figure 3.11: Hysteresis curves for different input frequencies Zhu and Rui, 2016 [41]

Chapter 4

Control of the piezoelectric actuator

In this chapter we present a first approach for using the proposed model to synthesize a nonlinear passivity based position controller for a class of piezoelectric actuator. The controller is designed starting from a nominal model which is obtained under the assumption that the electro-mechanical coupling is independent of the temperature. For this nominal model a control law which asymptotically stabilizes the closed-loop system at the desired dynamic equilibrium is proposed. In a second instance, the proposed model is obtained by perturbing the nominal model with the temperature dependent electro-mechanical coupling. Lyapunov perturbation theory is then used to show that under some general operation assumptions the proposed passivity based controller asymptotically stabilizes the closed-loop system. The control action can be interpreted in terms of damping/entropy injection with respect to the desired dynamic equilibrium.

4.1 Some preliminaries on stability

In this section, some fundamental theorems on Lyapunov stability are presented [14].

Theorem 4.1 *(Lyapunov's Stability Theorem) Let x^* be an equilibrium point and $D \subset \mathbb{R}^n$ be a domain containing x^*. Let $V : D \to \mathbb{R}$ be a continuously differentiable function such that satisfies*

1. $V(x) > 0, \forall x \in D - \{x^*\}$
2. $V(x^*) = 0$
3. $\dot{V}(x) \leq 0$

Then, x^* is stable in the sense of Lyapunov and $V(x)$ is denominated as Lyapunov function. Moreover if

$$\dot{V}(x) < 0$$

Then, x^* is asymptotically stable.

Theorem 4.2 *(LaSalle's Invariance Principle) Let $\Omega \subset D$ be a compact set that is positively invariant with respect to $\dot{x} = f(x)$. Let $V : D \to \mathbb{R}$ be a continuously differentiable function*

such that $\dot{V}(x) \leq 0$ in Ω. Let E be a set of all the points in Ω where $\dot{V}(x) = 0$. Let M be the largest invariant set in E. Then every solutions starting in Ω approaches M as $t \to \infty$.

Corollary 4.1 *Let x^* be an equilibrium point for $\dot{x} = f(x)$. Let $V : D \to \mathbb{R}$ be a continuously differentiable positive definite function on a domain D containing x^*, such that $\dot{V}(x) \leq 0$ in D. Let $S = \{x \in D \,|\, \dot{V}(x) = 0\}$ and suppose that no solution can stay identically in S, other than the solution $x(t) = x^*$. Then, the equilibrium point x^* is asymptotically stable.*

Lemma 4.1 *(Stability of Perturbed Systems) Consider the system*

$$\dot{x} = f(t, x) + g(t, x) \tag{4.1}$$

and $x = x^*$ be an uniformly asymptotically stable equilibrium point of the nominal system

$$\dot{x} = f(t, x) \tag{4.2}$$

suppose the nominal system has a definite, decrescent Lyapunov function $V(t, x)$ that satisfies

$$\frac{\partial V}{\partial t} + \frac{\partial V}{\partial x}^T f(t, x) \leq -W(x) \tag{4.3}$$

for all $(t, x) \in [0, \infty) \times D$ where $W(x)$ is positive definite and continuous. The derivative along the trajectories of (4.1) is given by

$$\begin{aligned} \dot{V}(t, x) &= \frac{\partial V}{\partial t} + \frac{\partial V}{\partial x}^T f(t, x) + \frac{\partial V}{\partial x}^T g(t, x) \\ &\leq -W(x) + \left\| \frac{\partial V}{\partial x}^T g(t, x) \right\| \end{aligned}$$

Then, if $W(x)$ satisfies

$$\left\| \frac{\partial V}{\partial x}^T g(t, x) \right\| < W(x) \tag{4.4}$$

the equilibrium point x^* is an uniformly asymptotically stable of the perturbed system (4.1).

Candidate Lyapunov Function for IPHS

Since the internal energy of the irreversible thermodynamic system does not have a strict minimum, a standard candidate Lyapunov function for control is the energy based availability function [15, 16]

Definition 4.1 *The energy based availability function is defined as*

$$A(x, x^*) = U(x) - U(x^*) - \frac{\partial U}{\partial x}(x^*)(x - x^*) \tag{4.5}$$

where $U(x)$ is the internal energy of the system and x^* is the desired equilibrium point of a thermodynamic variable x.

The availability function uses the convexity of the internal energy together with the assumption that one of the extensive variables is fixed, to construct a strictly convex extension which serves as Lyapunov function for a desired equilibrium point [18, 17]. We shall use this function as the Lyapunov closed-loop function for irreversible port-Hamiltonian system.

4.2 Control design

In this section we propose a control design based on two steps: In a first instance a PBC for a simplified nominal system is synthesized (see Figure 4.1a). The assumption used to formulate the nominal system is that the electro-mechanical coupling is independent of the temperature. Under this assumption a damping/entropy assignment controller which asymptotically stabilizes the nominal systems is derived using as candidate Lyapunov function an energy based availability function. In a second instance, proposed model of the piezo electric actuator is obtained by perturbing the nominal system with a temperature dependent electro-mechanical coupling (see Figure 4.1b). A perturbed system stability analysis is then performed under some general operation assumptions to show the asymptotic stability analysis of the proposed model.

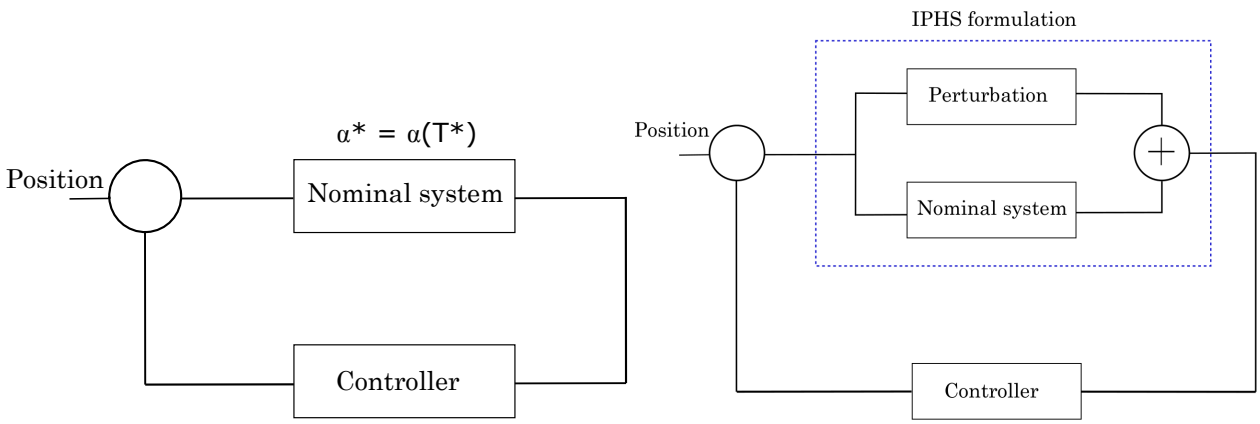

(a) Controller design for a nominal system (b) Stability analysis of a perturbed system

Figure 4.1: Strategy of control design

4.2.1 Characterization of equilibrium points

Let us characterize the admissible equilibrium(s) point(s) $x^* = (p^*, q^*, Q^*, \phi_1^*, \cdots, \phi_r^*, S^*)$ of the proposed piezoelectric model. These are given when the derivatives of the system in steady state are< equal to zero, that is $\dot{x} = 0$, for some constant inputs $u^* = (F_{ext}^*, V_{in}^*, T_e^*)$.

Proposition 4.1 *The admissible equilibrium points are*

$$x^* = \left(0, q_l + \tfrac{1}{k}\left(\alpha(T^*)V_{in}^* + F_{ext}^*\right), V_{in}^* C, 0, \cdots, 0, c_0 \ln\left(\tfrac{T^*}{T_0}\right)\right) \tag{4.6}$$

Proof. Recall that the state equations of the model are

$$\begin{aligned}
\dot{q} &= \frac{p}{M} \\
\dot{p} &= -k(q - q_l) - d\frac{p}{M} + \alpha(T)\frac{Q}{C} + F_{ext} \\
\dot{Q} &= \sum_{j=1}^{r} \frac{\phi_j}{L_j} - \alpha(T)\frac{p}{M} \\
\dot{\phi}_{L_j} &= V_{in} - \frac{Q}{C} - w_j\left(\frac{\phi_j}{L_j}, T\right) \\
\dot{S} &= \sum_{j=1}^{r} \sigma_{h_j} + \sigma_d + \lambda\left(\frac{T_e}{T} - 1\right)
\end{aligned}$$

starting with the state equation of $\dot{q}$ we can conclude that

$$\dot{q} = \frac{p^*}{M} = 0 \Rightarrow p^* = 0$$

replacing this result in the state equation of $\dot{Q}$ we can obtain

$$\dot{Q} = \sum_{j=1}^{r} \frac{\phi_j^*}{L_j} = 0$$

assuming that the temperature of the piezoelectric actuator is equal to the environment temperature, i.e. $T_e^* = T^*$, the state equation of $\dot{S}$ is

$$\dot{S} = \frac{1}{T^*}\left(\sum_{j=1}^{r} \frac{\phi_j^*}{L_j} w_j\left(\tfrac{\phi_j^*}{L_j}, T^*\right)\right) = 0 \Rightarrow \sum_{j=1}^{r} \frac{\phi_j^*}{L_j} w_j\left(\tfrac{\phi_j^*}{L_j}, T^*\right) = 0$$

recalling that $\sigma_{h_j} \geq 0$ for each value of j leads us to conclude that

$$\phi_j^* = 0, \quad \forall j$$

from the last two state equations $\dot{p}$ and $\dot{\phi}_j$

$$\dot{\phi}_j = V_{in}^* - \tfrac{Q^*}{C} = 0 \Rightarrow Q^* = V_{in}^* C$$

$$\dot{p} = -k(q^* - q_l) + \alpha(T^*)\frac{Q^*}{C} + F_{ext}^* = 0 \Rightarrow q^* = q_l + \frac{1}{k}\left(\alpha(T^*)V_{in}^* + F_{ext}^*\right)$$

and S^* is calculated from the constitutive equation $T(S) = T_0 e^{\frac{S}{c_0}}$

$$S^* = c_0 \ln\left(\frac{T^*}{T_0}\right)$$

Thus, the admissible equilibrium points are defined by (4.6). □

Consider the piezoelectric model described by Equations (3.33) - (3.37), the objective is to design a control law that asymptotically reaches an equilibrium point x^*. Lemma 4.1 shall be used in order to design the controller.

4.2.2 Control design of the nominal system

Define the following nominal system from the IPHS model of the piezoelectric actuator

$$\dot{q} = \frac{p}{M} \tag{4.7}$$

$$\dot{p} = -k(q - q_l) - d\frac{p}{M} + \alpha^* \frac{Q}{C} + F_{ext} \tag{4.8}$$

$$\dot{Q} = \sum_{j=1}^{r} \frac{\phi_j}{L_j} - \alpha^* \frac{p}{M} \tag{4.9}$$

$$\dot{\phi}_{L_j} = V_{in} - \frac{Q}{C} - w_j\left(\frac{\phi_j}{L_j}, T\right) \tag{4.10}$$

$$\dot{S} = \sum_{j=1}^{r} \sigma_{h_j} + \sigma_d + \lambda\left(\frac{T_e}{T} - 1\right) \tag{4.11}$$

where the electro-mechanical transducer ratio is a constant that depends on the temperature equilibrium point T^*, that is $\alpha(T^*) = \alpha^*$. We shall consider the following general operation assumptions.

Assumption 4.1

1. *The only control input is the voltage V_{in}.*
2. *The piezoelectric actuator is not under any external forces $F_{ext} = 0$.*
3. *We measure but not modify the environment temperature, this implies $T_e = T^*$.*

Proposition 4.2 *The control law*

$$V_{in} = \frac{Q^*}{C} \tag{4.12}$$

asymptotically stabilizes the nominal system (4.7) - (4.11) *at the equilibrium x^*.*

Proof. Select the following Lyapunov function candidate for the nominal system (4.7) - (4.11)

$$V(x) = \frac{1}{2}k(q - q^*)^2 + \frac{1}{2}\frac{p^2}{M} + \frac{1}{2}\frac{(Q - Q^*)^2}{C} + \frac{1}{2}\sum_{j=1}^{r}\frac{\phi_j^2}{L_j} + A(S) \tag{4.13}$$

where $V(x)$ is the sum of quadratic functions of the state and $A(S)$ that is the energy based availability function for the S component defined as

$$A(S) = f_h(S) - f_h(S^*) - T^*(S - S^*) \tag{4.14}$$

Then, from Equation (4.13) we proceed to calculate the derivative respect to time of $V(x)$ obtaining

$$\begin{aligned} \dot{V} = {} & k(q_l - q^*)\frac{p}{M} + \alpha^*\frac{Q^*}{C}\frac{p}{M} - \frac{T^*}{T}\left(\sum \frac{\phi_j}{L_j} w_j\left(\frac{\phi_j}{L_j}, T\right) + d\left(\frac{p}{M}\right)^2\right) \\ & + \left(V_{in} - \frac{Q^*}{C}\right)\sum \frac{\phi_j}{L_j} + (T - T^*)\lambda\left(\frac{T_e}{T} - 1\right) + F_{ext}\frac{p}{M} \end{aligned} \tag{4.15}$$

Considering Assumption 4.1 and the definition of the feasible equilibrium points in (4.6) (Proposition 4.1), we have that $q^* - q_l = \frac{1}{k}(\alpha^* \frac{Q^*}{C} + F^*_{ext})$. Thus, $\dot{V}$ is equal to

$$\dot{V}(x) = -\frac{T^*}{T}\left(\sum \frac{\phi_j}{L_j} w_j \left(\frac{\phi_j}{L_j}, T\right) + d\left(\frac{p}{M}\right)^2\right) + \left(V_{in} - \frac{Q^*}{C}\right)\sum \frac{\phi_j}{L_j} - (T - T^*)^2 \frac{\lambda}{T}$$

and using the control $V_{in} = \dfrac{Q^*}{C}$ the time variation of the Lyapunov candidate is

$$\dot{V}(x) = -T^* \sum_{j=1}^{r} \sigma_{h_j} - T^* \sigma_d - (T - T^*)^2 \frac{\lambda}{T} \leq 0 \tag{4.16}$$

Thus, the conditions from Theorem 4.1 are satisfied and we can conclude that the equilibrium point x^* is stable. Moreover, note that $\dot{V}(x) = 0$ only when $x = x^*$ then, from Corollary 4.1 the equilibrium point x^* is asymptotically stable. □

4.2.3 Control of the perturbed system

We shall perform the following physically based assumption which assures that when the system approaches the dynamic equilibrium it exhibits a linear behavior.

Assumption 4.2 *Suppose that near the equilibrium point, the absolute the difference between the temperature and its equilibrium satisfies the following inequality*

$$|T - T^*| \leq \varepsilon_d |p| + \sum_{j=1}^{r} \varepsilon_j \left|\frac{\phi_j}{L_j}\right| \tag{4.17}$$

where ε_d, ε_j are positive constants.

Note that Assumption 4.2 can be interpreted as follows. The difference to reach the equilibrium point of the temperature is bounded by the linear combination of the kinetic momentum p and magnetic flux of the inductors ϕ_j, indeed, (4.17) means that near the equilibrium, when the kinetic momentum and the magnetic flux approaches zero, the temperature approaches T^*.

The following proposition uses Lemma 4.1 to conclude about asymptotic stability of the proposed model.

Corollary 4.2 *The control law of Proposition 4.2 asymptotically stabilizes the IPHS formulation* (3.33) - (3.37) *within a region around the equilibrium point which depends on the electro-mechanical coupling function $\alpha(T)$.*

Proof. Until this point, we have found a Lyapunov function and designed a control law that stabilizes the nominal system at x^*. In the following we shall use Lemma 4.1 to show the asymptotic stability of the proposed model. To this end we look for a continuous positive function $W(x)$ that satisfies (4.3). From Equation (4.16) we have

$$\begin{aligned}\dot{V}(x) &= -T^* \sum_{j=1}^{r} \sigma_{h_j} - T^* \sigma_d - (T - T^*)^2 \frac{\lambda}{T} \\ &\leq -T^* \sum_{j=1}^{r} \sigma_{h_j} - T^* \sigma_d\end{aligned}$$

Thus, we can select $W(x)$ as

$$W(x) = T^* \left(\sum_{j=1}^{r} \sigma_{h_j} + \sigma_d \right) \tag{4.18}$$

Now we need to verify that the selected $W(x)$ satisfies the condition

$$\left\| \frac{\partial V}{\partial x}^T g(t,x) \right\| < W(x) \tag{4.19}$$

recall that $g(t,x)$ is

$$g(t,x) = \begin{bmatrix} 0 \\ \alpha(T)\frac{Q}{C} - \alpha^* \frac{Q}{C} \\ -\alpha(T)\frac{p}{M} + \alpha^* \frac{p}{M} \\ 0 \\ \vdots \\ 0 \end{bmatrix}$$

Then, using this and Assumption 3.2 led us to

$$\left\| \frac{\partial V}{\partial x} g(t,x) \right\| = \left| a_T (T - T^*) \frac{Q^*}{C} \frac{p}{M} \right| = \left| \frac{a_T Q^*}{CM} \right| |T - T^*| \, |p| \tag{4.20}$$

Considering Assumption 4.2, Equation (4.19) becomes

$$k_\alpha \left(\varepsilon_d |p|^2 + \sum_{j=1}^{r} \varepsilon_j \left| \frac{\phi_j}{L_j} \right| |p| \right) < T^* \left(\sum_{j=1}^{r} \sigma_{h_j} + \sigma_d \right) \tag{4.21}$$

where $k_\alpha = \left| \frac{a_T Q^*}{CM} \right|$. Hence, Lemma 4.1 is always fulfilled in a region sufficiently small around the equilibrium. The values of ε_d and ε_j will depend on the choice of the electro-mechanical coupling function $\alpha(T)$. Thus it is concluded that the control law (4.12) stabilizes the IPHS model of the piezoelectric actuator at the equilibrium point x^* asymptotically. □

Chapter 5

Conclusions

In this thesis work, an irreversible port-Hamiltonian system formulation for a class of piezoelectric actuator with non-negligible entropy increase has been proposed. The proposed model encompasses the hysteresis and the irreversible thermodynamic changes due to mechanical friction, electrical resistance and heat exchange between the actuator and the environment. The electromechanical dynamic of the actuator has been modeled using a non-linear resistive-capacitive-inductor circuit coupled with a mass-spring-damper system, while the non-linear hysteresis has been characterized using hysterons. The thermodynamic behavior of the model has been constructed by making the electro-mechanical coupling temperature dependent, and by characterizing the entropy produced by the irreversible phenomena. By means of numerical simulations it has been shown that the proposed model is capable of reproducing the expected behaviors and that it is in line with reported experimental results. It is interesting to notice that for the numerical simulations only two hysterons were used, strongly limiting the possible dynamics.

A first approach for using the proposed irreversible port-Hamiltonian model to synthesize a non-linear passivity based position controller for a class of piezoelectric actuator has been proposed. The controller is designed from a nominal model which is obtained under the assumption that the electro-mechanical transducer ratio is a constant. From this nominal model a control law that asymptotically stabilizes the closed-loop system at the desired equilibrium is proposed. Then, a perturbed system stability analysis is performed under some assumptions to show the asymptotic stability of the proposed model.

Future work will deal with control design using other techniques, for instance: interconnection and entropy rate assignment, deduce the number of hysterons to be used in the model and experimental validation.

Bibliography

[1] V. Duindam, A. Macchelli, S. Stramigioli, and H. Bruyninckx, *Modeling and control of complex physical systems: the port-Hamiltonian approach*. Springer Science & Business Media, 2009.

[2] R. Ortega, A. J. Van Der Schaft, I. Mareels, and B. Maschke, "Putting energy back in control," *IEEE Control Systems Magazine*, vol. 21, no. 2, pp. 18–33, 2001.

[3] R. Ortega, A. Van Der Schaft, B. Maschke, and G. Escobar, "Interconnection and damping assignment passivity-based control of port-controlled Hamiltonian systems," *Automatica*, vol. 38, no. 4, pp. 585–596, 2002.

[4] H. Ramirez, B. Maschke, and D. Sbarbaro, "Irreversible port-Hamiltonian systems: A general formulation of irreversible processes with application to the CSTR," *Chemical Engineering Science*, vol. 89, pp. 223–234, 2013.

[5] H. Ramirez, B. Maschke, and D. Sbarbaro, "Modelling and control of multi-energy systems: An irreversible port-Hamiltonian approach," *European journal of control*, vol. 19, no. 6, pp. 513–520, 2013.

[6] M. Rakotondrabe and Y. Le Gorrec, "Force control in piezoelectric microactuators using self scheduled H technique," *IFAC Proceedings Volumes*, vol. 43, no. 18, pp. 417–422, 2010.

[7] M. Goldfarb and N. Celanovic, "Modeling piezoelectric stack actuators for control of micromanipulation," *IEEE Control Systems Magazine*, vol. 17, no. 3, pp. 69–79, 1997.

[8] M. Rakotondrabe, "Bouc-Wen modeling and inverse multiplicative structure to compensate hysteresis nonlinearity in piezoelectric actuators," *IEEE Transactions on Automation Science and Engineering*, vol. 8, no. 2, pp. 428–431, 2010.

[9] H. Ghafarirad, S. Rezaei, A. A. Sarhan, and M. Zareinejad, "Continuous dynamic modelling of bimorph piezoelectric cantilevered actuators considering hysteresis effect and dynamic behaviour analysis," *Mathematical and Computer Modelling of Dynamical Systems*, vol. 21, no. 2, pp. 130–152, 2015.

[10] D. Karnopp, "Computer models of hysteresis in mechanical and magnetic components," *Journal of the Franklin Institute*, vol. 316, no. 5, pp. 405–415, 1983.

[11] N. R. Calchand, *Modeling and control of magnetic shape memory alloys using port hamiltonian framework*. Theses, Université de Franche-Comté, June 2014.

[12] H. Ramirez, Y. Le Gorrec, and N. Calchand, "Irreversible port-Hamiltonian formulation of non-isothermal electromechanical systems with hysteresis," *IFAC-PapersOnLine*, vol. 51, no. 3, pp. 19–24, 2018.

[13] A. van der Schaft, *L2-gain and passivity techniques in nonlinear control*, vol. 2. Springer, 2000.

[14] H. Khalil, *Nonlinear Systems*. Pearson Education, Prentice Hall, 2002.

[15] A. A. Alonso and B. E. Ydstie, "Stabilization of distributed systems using irreversible thermodynamics," *Automatica*, vol. 37, no. 11, pp. 1739–1755, 2001.

[16] B. E. Ydstie, "Passivity based control via the second law," *Computers & chemical engineering*, vol. 26, no. 7-8, pp. 1037–1048, 2002.

[17] H. Ramirez, Y. Le Gorrec, B. Maschke, and F. Couenne, "On the passivity based control of irreversible processes: A port-Hamiltonian approach," *Automatica*, vol. 64, pp. 105 – 111, 2016.

[18] I. Villalobos, H. Ramírez, and Y. Le Gorrec, "Energy shaping plus damping injection of irreversible port hamiltonian systems," *IFAC-PapersOnLine*, vol. 53, no. 2, pp. 11539–11544, 2020.

[19] X. Ye and Z.-j. Zhang, "Piezoelectric-ceramic-based microgrippers in micromanipulation," *Piezoelectric Ceramics*, pp. 253–268, 2010.

[20] Y. Haddab, N. Chaillet, and A. Bourjault, "A microgripper using smart piezoelectric actuators," in *Proceedings. 2000 IEEE/RSJ International Conference on Intelligent Robots and Systems (IROS 2000)(Cat. No. 00CH37113)*, vol. 1, pp. 659–664, IEEE, 2000.

[21] J. Agnus, J.-M. Breguet, N. Chaillet, O. Cois, P. De Lit, A. Ferreira, P. Melchior, C. Pellet, and J. Sabatier, "A smart microrobot on chip: design, identification and modeling," in *Proceedings 2003 IEEE/ASME International Conference on Advanced Intelligent Mechatronics (AIM 2003)*, vol. 2, pp. 685–690, IEEE, 2003.

[22] X. Huang, J. Cai, M. Wang, and X. Lv, "A piezoelectric bimorph micro-gripper with micro-force sensing," in *2005 IEEE International Conference on Information Acquisition*, pp. 5–pp, IEEE, 2005.

[23] M. Rakotondrabe, Y. Haddab, and P. Lutz, "Development, Modeling, and Control of a Micro-/Nanopositioning 2-DOF Stick-Slip Device," *IEEE/ASME Transactions on Mechatronics*, vol. 14, no. 6, pp. 733–745, 2009.

[24] P. Ge and M. Jouaneh, "Modeling hysteresis in piezoceramic actuators," *Precision engineering*, vol. 17, no. 3, pp. 211–221, 1995.

[25] Ping Ge and Musa Jouaneh, "Tracking control of a piezoceramic actuator," *IEEE Transactions on Control Systems Technology*, vol. 4, no. 3, pp. 209–216, 1996.

[26] T.-G. Zsurzsan, M. A. Andersen, Z. Zhang, and N. A. Andersen, "Preisach model of hysteresis for the Piezoelectric Actuator Drive," in *IECON 2015-41st Annual Conference of the IEEE Industrial Electronics Society*, pp. 002788–002793, IEEE, 2015.

[27] D. Habineza, M. Rakotondrabe, and Y. Le Gorrec, "Bouc-Wen modeling and feedforward control of multivariable hysteresis in piezoelectric systems: Application to a 3-DoF piezotube scanner," *IEEE Transactions on Control Systems Technology*, vol. 23, no. 5, pp. 1797–1806, 2015.

[28] J. B. Liseli, J. Agnus, P. Lutz, and M. Rakotondrabe, "An overview of piezoelectric self-sensing actuation for nanopositioning applications: Electrical circuits, displacement, and force estimation," *IEEE Transactions on Instrumentation and Measurement*, vol. 69, no. 1, pp. 2–14, 2019.

[29] M. Rakotondrabe, C. Clévy, and P. Lutz, "Hinf deflection control of a unimorph piezoelectric cantilever under thermal disturbance," in *2007 IEEE/RSJ International Conference on Intelligent Robots and Systems*, pp. 1190–1195, IEEE, 2007.

[30] M. Rakotondrabe and I. A. Ivan, "Development and dynamic modeling of a new hybrid thermopiezoelectric microactuator," *IEEE Transactions on Robotics*, vol. 26, no. 6, pp. 1077–1085, 2010.

[31] D. Habineza, M. Zouari, M. Hammouche, Y. Le Gorrec, and M. Rakotondrabe, "Characterization and modeling of the temperature effect on the piezoelectric tube actuator," *IFAC-PapersOnLine*, vol. 49, no. 21, pp. 354–360, 2016.

[32] M. Al Janaideh, M. Al Saaideh, and M. Rakotondrabe, "Temperature dependent hysteresis modeling of a piezotube actuator using elman neural network," in *Dynamic Systems and Control Conference*, vol. 59148, p. V001T09A004, American Society of Mechanical Engineers, 2019.

[33] A. Meitzler, H. Tiersten, A. Warner, D. Berlincourt, G. Couqin, and F. Welsh III, "IEEE standard on Piezoelectricity," 1988.

[34] K. Kuhnen and H. Janocha, "Inverse feedforward controller for complex hysteretic nonlinearities in smart-material systems," *Control and Intelligent systems*, vol. 29, no. 3, pp. 74–83, 2001.

[35] A. J. van der Schaft, "Port-hamiltonian systems: network modeling and control of nonlinear physical systems," in *Advanced dynamics and control of structures and machines*, pp. 127–167, Springer, 2004.

[36] B. M. Maschke, A. J. Van Der Schaft, and P. C. Breedveld, "An intrinsic hamiltonian formulation of network dynamics: Non-standard poisson structures and gyrators," *Journal of the Franklin institute*, vol. 329, no. 5, pp. 923–966, 1992.

[37] H. B. Callen, "Thermodynamics and an introduction to thermostatistics," 1998.

[38] H. Ramírez, B. Maschke, and D. Sbárbaro, "On the hamiltonian formulation of the cstr," in *49th IEEE Conference on Decision and Control (CDC)*, pp. 3301–3306, IEEE, 2010.

[39] D. Eberard, B. Maschke, and A. Van Der Schaft, "An extension of hamiltonian systems to the thermodynamic phase space: Towards a geometry of nonreversible processes," *Reports on mathematical physics*, vol. 60, no. 2, pp. 175–198, 2007.

[40] I. Thorlabs, "Piezoelectric Bimorph,." `https://www.thorlabs.com/drawings/5b692d43c7477ea-66DBD8C4-D071-BE7A-2F7780CE82D7A43F/PB4NB2W-SpecSheet.pdf/`, 6 2020. CTN010296-S01, Rev C.

[41] W. Zhu and X.-T. Rui, "Hysteresis modeling and displacement control of piezoelectric actuators with the frequency-dependent behavior using a generalized bouc–wen model," *Precision Engineering*, vol. 43, pp. 299–307, 2016.

[42] O. Aljanaideh, M. Al Janaideh, and M. Rakotondrabe, "Inversion-free feedforward dynamic compensation of hysteresis nonlinearities in piezoelectric micro/nano-positioning actuators," in *2015 IEEE International Conference on Robotics and Automation (ICRA)*, pp. 2673–2678, IEEE, 2015.